

DYNAMICAL PRUNING OF BINARY TREES WITH APPLICATIONS TO 1D BALLISTIC ANNIHILATION

MAXIM ARNOLD, YEVGENIY KOVCHegov, AND ILYA ZALIAPIN

ABSTRACT. We introduce *generalized dynamical pruning* on rooted binary trees with edge lengths. The pruning removes parts of a tree T , starting from the leaves, according to a pruning function defined on subtrees within T . The generalized pruning encompasses a number of discrete and continuous pruning operations, including the tree erasure and Horton pruning. The main result is invariance of a finite critical binary Galton-Watson tree with exponential edge lengths with respect to the generalized dynamical pruning for an arbitrary admissible pruning function. The second part of the paper examines the 1-D ballistic annihilation dynamics $A + A \rightarrow \emptyset$ for the initial velocity that alternates between the values of ± 1 . The model dynamics is shown to be equivalent to a generalized dynamical pruning of the level set tree of the model potential (integral of velocity), with the pruning function equal to the total tree length. This equivalence allows us to construct a complete description of the annihilation dynamics for the initial velocity that alternates between the values of ± 1 at the epochs of a stationary Poisson process.

CONTENTS

1. Introduction	2
2. Generalized dynamical pruning	5
2.1. Trees	5
2.2. Generalized dynamical pruning	7
2.3. Relation to other generalizations of pruning	12
2.4. Invariance with respect to generalized dynamical pruning	13
3. Dynamical pruning for exponential critical Galton-Watson trees	14
3.1. Harris path	15
3.2. Level set tree	15
3.3. Exponential critical binary Galton-Watson tree $\text{GW}(\lambda)$	18
3.4. Length of a random tree $\text{GW}(\lambda)$	19
3.5. Prune invariance of $\text{GW}(\lambda)$	21
4. Continuum ballistic annihilation model, $A + A \rightarrow \emptyset$	26

4.1.	Continuum model, sinks, and shock trees	26
4.2.	Basic constraints on ballistic annihilation dynamics	28
4.3.	Piece-wise linear potential with unit slopes	29
4.4.	Ballistic annihilation of a unit-slope potential	38
5.	Ballistic annihilation of an exponential excursion	42
6.	Random sink in an infinite exponential potential	49
7.	Discussion	52
	Acknowledgements	54
	References	54

1. INTRODUCTION

Pruning of tree graphs is a natural operation that induces a contracting map [21] on a suitable space of trees, with the empty tree ϕ as the fixed point. Examples of prunings studied in probability literature include erasure from leaves at unit speed [29, 15, 10], cutting the leaves [9, 24, 26], and eliminating nodes/edges at random [3, 1]. We consider here erasure of a tree from the leaves at a non-constant tree-dependent rate. Specifically, we introduce *generalized dynamical pruning* $\mathcal{S}_t(\varphi, T)$ of a rooted tree T that eliminates all subtrees $\Delta_{x,T}$ (defined as the points descendant to point x in T) for which the value of a function $\varphi(\Delta_{x,T})$ is below t (see Section 2.2 for a formal definition). The generalized dynamical pruning encompasses a number of discrete and continuous pruning operations, depending on a choice of function φ . For instance, the tree erasure from leaves at unit speed [29, 15] corresponds to the pruning function $\varphi(T)$ equal to the height of T ; and the Horton pruning [9, 26] corresponds to $\varphi(T)$ equal to the Horton-Strahler order of T . For most selections of $\varphi(T)$, the map induced by the generalized dynamical pruning does not have a semi-group property, which distinguishes it from the operations studied in the literature. Our main result (Section 3.5, Theorem 2) establishes invariance of the space of finite critical binary Galton-Watson trees with i.i.d. exponential edge lengths with respect to the generalized dynamical pruning, independently of (an admissible) pruning function. The invariance includes scaling of the edge lengths by the scaling constant equal to the survival probability $\mathbf{P}(\mathcal{S}_t(\varphi, T) \neq \phi)$. The explicit form of the survival probability is established in Theorem 3 for pruning by tree height (erasure from leaves at unit speed), by Horton order, and by tree length. The generalized prune invariance unifies several known invariance results (e.g., [29, 9]) and suggests a framework for studying diverse problem-specific pruning operations.

As a notable application, we consider the 1-D ballistic annihilation model, traditionally denoted $A + A \rightarrow \emptyset$. This model describes the dynamics of particles on a real line: a particle with Lagrangian coordinate x moves with the velocity $v(x, 0)$ until it collides with another particle, at which moment both particles annihilate, hence the model notation. The annihilation dynamics appears in chemical kinetics and bimolecular reactions; see [13, 5, 7, 32, 12, 6, 14, 8, 27, 34]. The annihilation dynamics produces *sinks* (*shocks*) that correspond to the collisions of individual particles with consequent annihilation. The moving *shock waves* represent the *sinks* that aggregate the annihilated particles and hence accumulate the mass of the media. Dynamics of these sinks resembles a coalescent process that generates a tree structure for their trajectories. The dynamics of a ballistic annihilation model with two coalescing sinks is illustrated in Fig. 1.

We consider here an initial velocity field $v(x, 0)$ that alternates between the values ± 1 , as illustrated in Fig. 2. Equivalently, we work with potential velocity field $v(x, t) = -\partial_x \psi(x, t)$ where the initial potential $\psi(x, 0)$ is a piece-wise linear continuous function with slopes ± 1 . This choice corresponds to a particularly tractable structure of the shock wave tree, which is completely described in this work. Specifically, the sinks may only emerge at $t = 0$ at the local minima of the potential $\psi(x, 0)$. The sinks move and merge to create a shock wave tree that coincides with the level set tree $T = \text{LEVEL}(\psi(x, 0))$ of the initial potential (Section 4.3, Theorem 4). The main application result (Section 4.4, Theorem 5) states that the ballistic annihilation dynamics in this case is equivalent to the generalized dynamical pruning of the shock wave tree with pruning function $\varphi(\tau)$ equal to the total length of τ . The pruned tree in this construction describes the potential restricted to the domain of particles that did not annihilate until instant t . To retain information about sinks and empty intervals, we equip a tree with *massive points*, placed at the tree *cuts* – the boundary of the pruned tree parts (Section 4.4, Definition 4). A complete description of ballistic annihilation dynamics is then given in terms of mass-equipped trees, which involves a suitably modified definition of pruning (Section 4.4). In particular, we establish a one-to-one correspondence between pruned mass-equipped trees and time-advanced potentials $\psi(x, t)$ with massive sinks (Section 4.4, Constructions 1, 2). Theorem 6 describes the ballistic annihilation dynamics for the initial velocity field that alternates between ± 1 at epochs of a stationary Poisson point process on \mathbb{R} . The respective potential corresponds to the Harris path of a critical binary Galton-Watson tree with i.i.d. exponential edge lengths. This equivalence allows one to use a suit of results available for the exponential

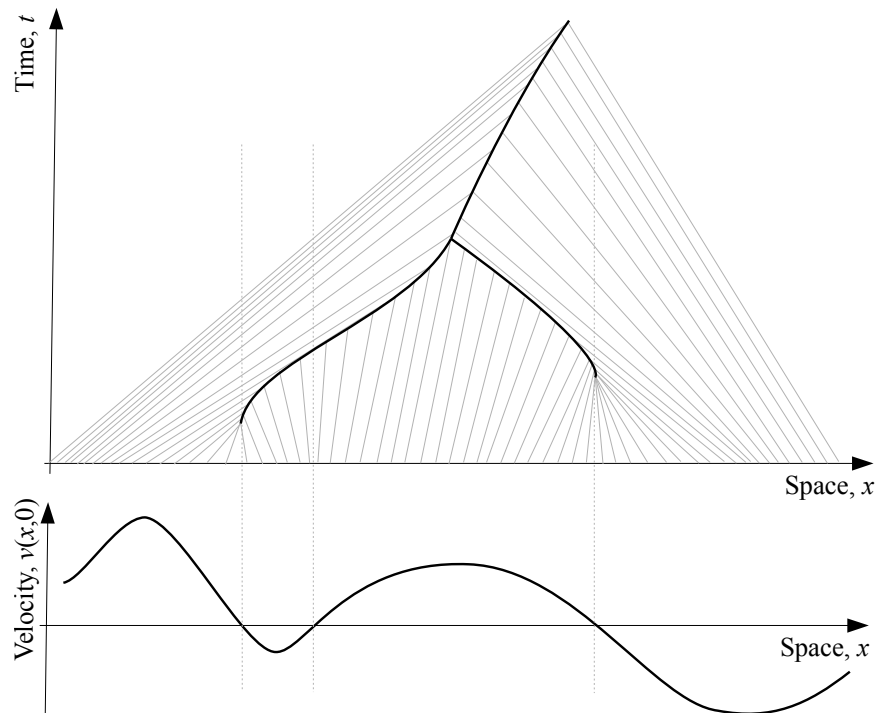


FIGURE 1. Ballistic annihilation model: an illustration. A particle with Lagrangian coordinate x moves with velocity $v(x, 0)$ until it collides with another particle and annihilates. (Bottom panel): Initial velocity $v(x, 0)$. (Top panel): The space-time portrait of the system. The trajectories of selected particles are depicted by gray thin lines. The shock wave that describes the motion and coalescence of sinks is shown by solid black line. The sink trajectory forms an inverted Y-shaped tree. Vertical dashed lines show the time instants when the initial velocity changes sign.

Galton-Watson tree to study the ballistic annihilation; in particular, this connects the ballistic annihilation dynamics with the invariance results of Theorems 2, 3. We use this connection to derive the time-dependent mass distribution of a random sink in an infinite potential (Section 6, Theorem 8).

The rest of the paper is organized as follows. The generalized dynamical pruning is introduced in Section 2. Section 3 collects necessary results on level set trees and proves the invariance theorems for critical binary Galton-Watson trees with i.i.d. exponential edge

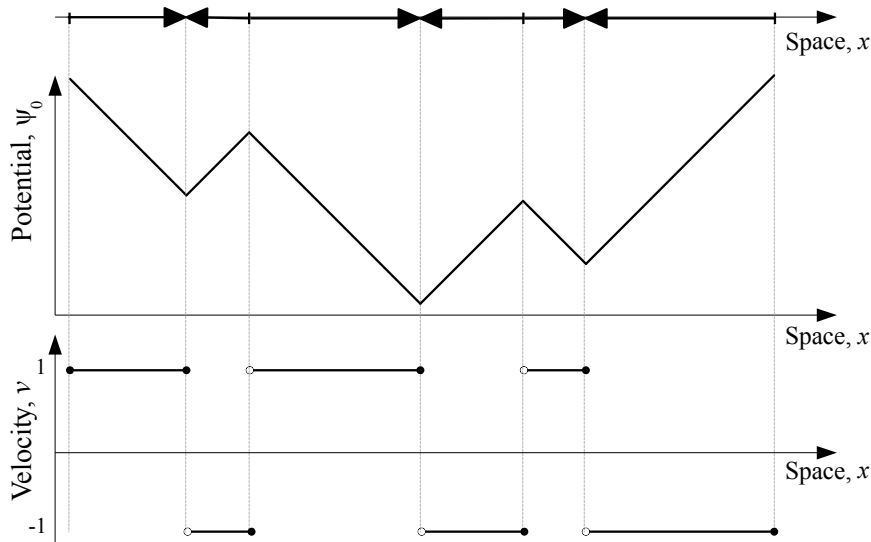


FIGURE 2. Piece-wise linear unit slope potential: an illustration. (Top): Arrows indicate alternating directions of particle movement on an interval in \mathbb{R} . (Middle): Potential $\Psi_0(x)$ is a piece-wise linear unit slope function. (Bottom): Particle velocity alternates between values ± 1 within consecutive intervals.

lengths. The shock wave tree for the dynamics of 1-D ballistic annihilation $A + A \rightarrow \emptyset$ with piece-wise unit slope potential is analyzed in Section 4. Sections 5,6 examine a unit slope potential with exponential segments durations (Poisson epoch velocity alterations), for a finite and infinite domain, respectively. Section 7 concludes.

2. GENERALIZED DYNAMICAL PRUNING

2.1. Trees. Consider a space $\mathcal{L}_{\text{plane}}$ of finite unlabeled rooted reduced binary trees with edge lengths and planar embedding. The space includes the *empty tree* ϕ comprised of a root vertex and no edges. A binary tree is called *rooted* if one of its vertices of degree 1 or 2 is selected as the tree root ρ . The existence of a root vertex imposes the parent-offspring relation between each pair of connected vertices in a tree $T \in \mathcal{L}_{\text{plane}}$: the one closest to the root is called *parent*, and the other – *offspring*. The tree root is the only vertex that does not have a parent. Formally, a binary tree $T = \rho \cup \{v_i, e_i\}_{1 \leq i \leq \#T}$ is comprised of the root ρ and a collection of non-root vertices v_i , each of which is connected to its unique parent $v_{\text{parent}(i)}$ by the parental edge e_i , $1 \leq i \leq \#T$. Here $\#T$ denotes the number of non-root vertices,

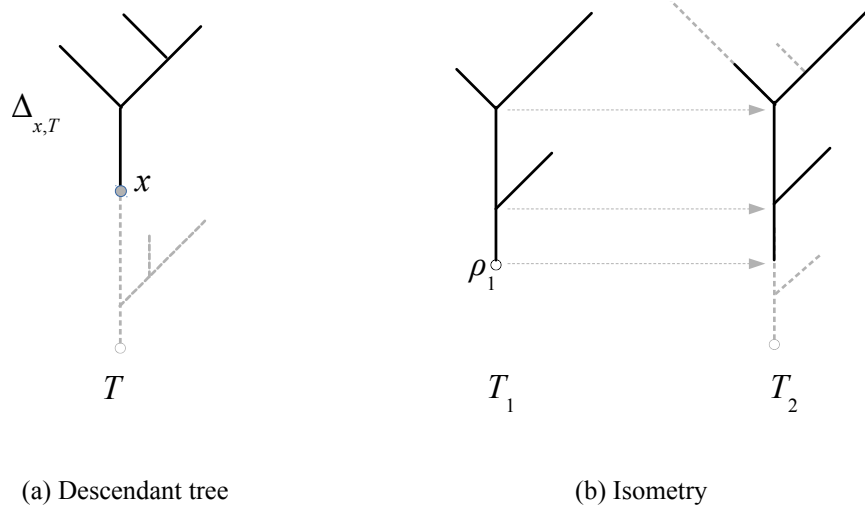


FIGURE 3. Descendant subtree and tree isometry: an illustration. (a) Subtree $\Delta_{x,T}$ (solid black lines) descendant to a point x (gray circle) in a tree T (union of dashed gray and solid black lines). (b) Isometry of trees. Tree T_1 (left) is mapped to tree T_2 (right). The image of T_1 within T_2 is shown by black lines, the rest of T_2 is shown by dashed gray lines. Here, tree T_1 is less than tree T_2 , $T_1 \leq T_2$.

equal to the number of edges, in a tree T . Unless indicated otherwise, the vertices are indexed in order of the depth-first search, starting from the root. A tree is called *reduced* if it has no vertices of degree 2, with the root as the only possible exception. The operation of *series reduction* removes each degree-two non-root vertex by merging its adjacent edges into one and adding the respective lengths. Planar embedding is equivalent to introducing a relative orientation (right/left) for every pair of siblings.

A rooted tree is called *planted* if its root has degree 1; in this case the only edge connected to the root is called *stem*. Otherwise the root has degree 2 and a tree is called *stemless*. We denote by $\mathcal{L}_{\text{plane}}^{\downarrow}$ and $\mathcal{L}_{\text{plane}}^{\uparrow}$ the subspaces of planted and stemless trees, respectively. Hence $\mathcal{L}_{\text{plane}} = \mathcal{L}_{\text{plane}}^{\downarrow} \cup \mathcal{L}_{\text{plane}}^{\uparrow}$ and $\mathcal{L}_{\text{plane}}^{\downarrow} \cap \mathcal{L}_{\text{plane}}^{\uparrow} = \emptyset$. Fig. 4 shows examples of a planted and a stemless tree. Most of our discussion in this work refers to planted trees.

Let $l_T = (l_1, \dots, l_{\#T})$ be the vector of edge lengths. The length of a tree T is the sum of the lengths of its edges:

$$\text{LENGTH}(T) = \sum_{i=1}^{\#T} l_i.$$

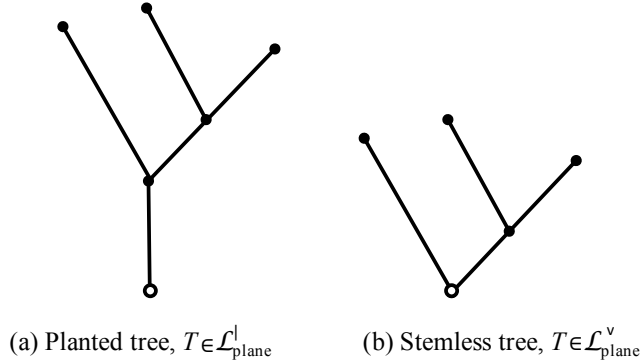


FIGURE 4. Examples of planted (a) and stemless (b) trees.

A tree $T \in \mathcal{L}_{\text{plane}}$ is naturally equipped with a length metric $d(x, y)$ for points $x, y \in T$. The distance $d(x, y)$ equals the length of the minimal path within T between x and y . The height of a tree T is the maximal distance between the root and a vertex:

$$\text{HEIGHT}(T) = \max_{1 \leq i \leq \#T} d(v_i, \rho).$$

Sometimes we focus on the combinatorial tree $\text{SHAPE}(T)$, which retains the branching structure of T while omitting its edge lengths and embedding. Similarly, $\text{P-SHAPE}(T)$ retains the branching structure of T and planar embedding, and omits the edge length information. The space of finite unlabelled rooted reduced binary planted combinatorial (planar) trees is denoted by \mathcal{T} ($\mathcal{T}_{\text{plane}}$).

2.2. Generalized dynamical pruning. Given a tree $T \in \mathcal{L}_{\text{plane}}$ and a point $x \in T$, let $\Delta_{x,T}$ be the *descendant tree* of x : it is comprised of all points of T descendant to x , including x ; see Fig. 3a. Then $\Delta_{x,T}$ is itself a tree in $\mathcal{L}_{\text{plane}}$ with root at x . Let (T_1, d) and (T_2, d) be two metric rooted trees, and let ρ_1 denote the root of T_1 . A function $f : (T_1, d) \rightarrow (T_2, d)$ is said to be an *isometry* if $\text{Image}[f] \subseteq \Delta_{f(\rho_1), T_2}$ and for all pairs $x, y \in T_1$,

$$d(f(x), f(y)) = d(x, y).$$

The tree isometry is illustrated in Fig. 3b. We use the isometry to define a *partial order* in the space $\mathcal{L}_{\text{plane}}$ as follows. We say that T_1 is *less than or equal to* T_2 and write $T_1 \leq T_2$ if and only if there is an isometry $f : (T_1, d) \rightarrow (T_2, d)$. The relation \leq is a partial order as it satisfies the reflexivity, antisymmetry, and transitivity conditions. Moreover, a variety of other properties of this partial order can be observed, including order denseness and semi-continuity.

We say that a function $\varphi : \mathcal{L}_{\text{plane}} \rightarrow \mathbb{R}$ is *monotone non-decreasing* with respect to the partial order \leq if $\varphi(T_1) \leq \varphi(T_2)$ whenever $T_1 \leq T_2$. Consider a monotone non-decreasing function $\varphi : \mathcal{L}_{\text{plane}} \rightarrow \mathbb{R}^+$. We define the *generalized dynamical pruning* operator $\mathcal{S}_t(\varphi, T) : \mathcal{L}_{\text{plane}} \rightarrow \mathcal{L}_{\text{plane}}$ induced by φ at any $t \geq 0$ as

$$\mathcal{S}_t(\varphi, T) := \rho \cup \left\{ x \in T \setminus \rho : \varphi(\Delta_{x,T}) \geq t \right\}.$$

Informally, the operator \mathcal{S}_t cuts all subtrees $\Delta_{x,T}$ for which the value of φ is below threshold t , and always keeps the tree root. Extending the partial order to $\mathcal{L}_{\text{plane}}$ by assuming $\phi \leq T$ for all $T \in \mathcal{L}_{\text{plane}}$, we observe for any $T \in \mathcal{L}_{\text{plane}}$ that $\mathcal{S}_s(T) \leq \mathcal{S}_t(T)$ whenever $s \geq t$.

The dynamical pruning operator \mathcal{S}_t encompasses and unifies a range of problems, depending on a choice of φ , as we illustrate in the following examples.

Example 1 (Tree height). Let the function $\varphi(T)$ equal the height of tree T :

$$(1) \quad \varphi(T) = \text{HEIGHT}(T).$$

In this case the operator \mathcal{S}_t satisfies **continuous semigroup property**:

$$\mathcal{S}_t \circ \mathcal{S}_s = \mathcal{S}_{t+s} \quad \text{for any } t, s \geq 0.$$

It coincides with the continuous pruning (tree erasure) studied in Neveu [29], who established invariance of a critical and sub-critical binary Galton-Watson processes with i.i.d. exponential edge lengths with respect to this operation.

It is readily seen that for a coalescent process, the dynamical pruning \mathcal{S}_t of the corresponding coalescent tree with $\varphi(T)$ as in (1) replicates the coalescent process.

Example 2 (Horton-Strahler order). Let the function $\varphi(T) + 1$ equal the Horton-Strahler order $\mathbf{k}(T)$ of a tree T :

$$(2) \quad \varphi(T) = \mathbf{k}(T) - 1.$$

The Horton-Strahler order [31, 9, 23] is closely related to the operation \mathcal{R} of leaf pruning with consecutive series reduction in a planted rooted tree. This operation is known as *Horton pruning*; it is illustrated in Fig. 5. The pruning induces a contracting map on $\mathcal{L}_{\text{plane}}$. The trajectory of each tree T under $\mathcal{R}(\cdot)$ is uniquely determined and finite:

$$(3) \quad T \equiv \mathcal{R}^0(T) \rightarrow \mathcal{R}^1(T) \rightarrow \dots \rightarrow \mathcal{R}^k(T) = \phi,$$

with the empty tree ϕ as the (only) fixed point [26]. The Horton-Strahler order $k(T)$ of a planted tree from $\mathcal{L}_{\text{plane}}^{\downarrow}$ is the minimal number of prunings necessary to eliminate a tree T . The Horton-Strahler order $k(T)$ of an unplanted tree from $\mathcal{L}_{\text{plane}}^{\vee}$ is the minimal number of prunings necessary to eliminate a tree T plus one. The Horton-Strahler order is also known as the *register number* [17], as it equals the minimum number of memory registers necessary to evaluate an arithmetic expression described by a tree T .

With the choice (2) the dynamical pruning operator coincides with the Horton pruning: $\mathcal{S}_t = \mathcal{R}^{|t|}$. It is readily seen that \mathcal{S}_t satisfies **discrete semigroup property**:

$$\mathcal{S}_t \circ \mathcal{S}_s = \mathcal{S}_{t+s} \text{ for any } t, s \in \mathbb{N}_0.$$

It has been shown in [9] that a critical binary Galton-Watson tree is invariant with respect to Horton pruning; moreover, this is the only prune-invariant distribution from the Galton-Watson family. Study [26] introduced a one-parameter family of prune-invariant trees, which includes critical binary Galton-Watson distribution as a special case. The Horton prune invariance is also empirically found in multiple observed and modeled systems (e.g., [31, 36, 37]).

A widespread empirical constraint related to the Horton-Strahler orders is so-called *Horton law* – a geometric decay of the number of branches of a given order in a finite tree; see [22, 31, 35, 11, 25] and references therein. Sufficient conditions for the Horton law in an asymptotically increasing tree were found in [23], hence providing rigorous foundations for the celebrated regularity that has escaped a formal explanation for a long time. A weak form of Horton law was proved for Kingman coalescent and the level set tree of a sequence of i.i.d. random variables [24].

Example 3 (Total tree length). Let the function $\varphi(T)$ equal the total lengths of T :

$$(4) \quad \varphi(T) = \text{LENGTH}(T).$$

The dynamical pruning by the tree length is illustrated in Fig. 6 for a Y-shaped tree that consists of three edges.

Importantly, in this case \mathcal{S}_t **does not satisfy** the semigroup property. To see this, consider an internal vertex point $x \in T$ (see Fig. 6, where the only internal vertex is marked by a gray ball). Then $\Delta_{x,T}$ consists of point x as its root, the left subtree of length a and the right subtree of length b . Observe that the whole left subtree is pruned away by time a , and the whole right subtree is pruned away by time b .

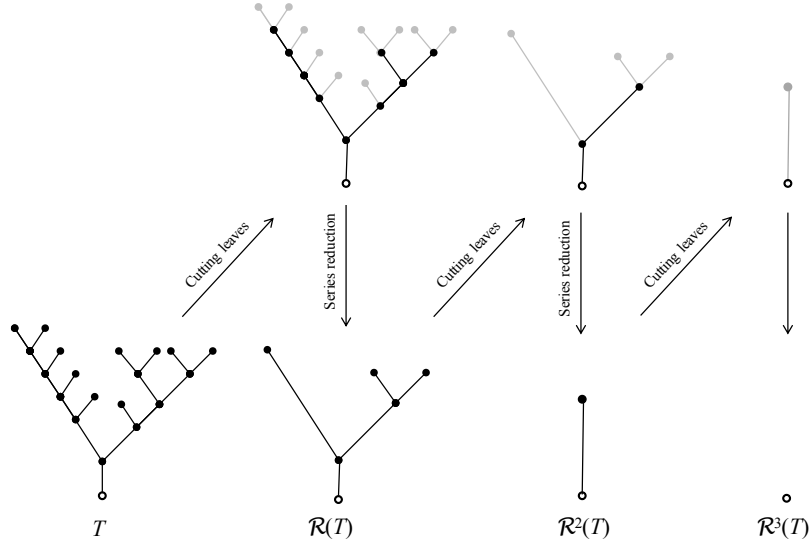


FIGURE 5. Horton pruning and Horton-Strahler ordering: an example. The order of the tree is $k(T) = 3$, since the tree T is eliminated in three prunings. Each pruning consists of cutting leaves (top row) and consecutive series reduction (bottom row). The pruning trajectory $T \rightarrow \mathcal{R}(T) \rightarrow \mathcal{R}^2(T) \rightarrow \mathcal{R}^3(T) = \phi$ is shown in the bottom row of panels.

However, since

$$\varphi(\Delta_{x,T}) = \text{LENGTH}(\Delta_{x,T}) = a + b,$$

the junction point x will not be pruned until time instant $a + b$. Thus, x will be a leaf of $\mathcal{S}_t(\varphi, T)$ for all t such that

$$\max\{a, b\} \leq t \leq a + b.$$

This situation corresponds to Stage IV in Fig. 6, where each of the left and right subtrees stemming from point x , marked by a gray ball, consists of a single edge.

The semigroup property in this example can be introduced by considering **mass-equipped trees**. Informally, we replace each pruned subtree τ of T with a point of mass equal to the total length of τ . The information encoded in the massive points allows one to reconstruct some of the information lost during the pruning process, and hence establish the semigroup property. Specifically, by time a , the pruned away left subtree turns into a massive point of mass a attached to x on the left side. Similarly, by time b , the pruned away right subtree turns into a massive point of mass b attached to x on the right side.

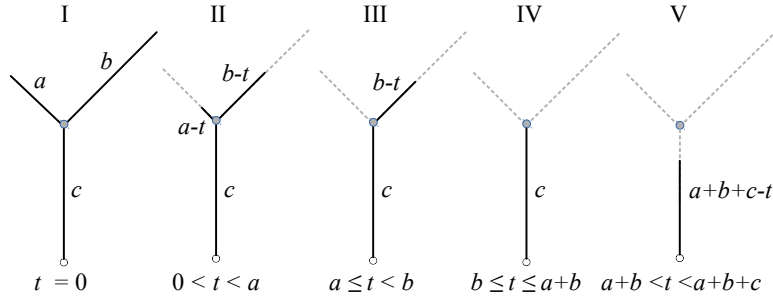


FIGURE 6. Pruning by tree length: an illustration. Figure shows five generic stages in the dynamical pruning of a Y-shaped tree T , with pruning function $\varphi(T) = \text{LENGTH}(T)$. The pruned tree \mathcal{S}_t is shown by solid black lines; the pruned parts of the initial tree are shown by dashed gray lines.

Stage I: Initial tree T consists of three edges, with lengths a, b, c indicated in the panel; without loss of generality we assume $a < b$.

Stage II: For any $t < a$ the pruned tree \mathcal{S}_t has a Y-shaped form with leaf edges truncated by t .

Stage III: For any $a \leq t < b$ the pruned tree \mathcal{S}_t consists of a single edge of length $c + b - t$.

Stage IV: For any $b \leq t \leq a + b$ the pruned tree \mathcal{S}_t consists of a single edge of length c . Notice that during this stage the tree \mathcal{S}_t does not change with t ; this loss of memory causes the process to violate the semigroup property.

Stage V: For any $a + b < t < a + b + c$ the pruned tree \mathcal{S}_t consists of a single edge of length $a + b + c - t$.

For $\max\{a, b\} \leq t \leq a + b$, the construction keeps track of the quantity $a + b - t$ associated with point x , and when the quantity $a + b - t$ decreases to 0, the two massive points coalesce into one. If a single massive point seats at a leaf, its mass is t . If a double massive point seats at a leaf, further pruning of the leaf's parental edge is prevented until the two massive points coalesce. Keeping track of all such quantities makes \mathcal{S}_t satisfy the continuous semigroup property. This construction is formally introduced in Section 4.

Notably, in this case the pruning operator \mathcal{S}_t coincides with the potential dynamics of continuum mechanics formulation of the 1-D ballistic annihilation model, $A + A \rightarrow \emptyset$, as discussed below in Section 4.

Example 4 (Number of leaves). Let the function $\varphi(T)$ equal the number of leaves in a tree T . This choice is closely related to the mass-conditioned dynamics of an aggregation process. Specifically, consider N singletons (particles with unit mass) that appear in a system at

instants $t_n \geq 0$, $1 \leq n \leq N$. The existing clusters merge into consecutively larger clusters by pair-wise mergers. The cluster mass is additive: a merger of two clusters of masses i and j results in a cluster of mass $i + j$. We consider a time-oriented tree T that describes this process. The tree T has N leaves and $(N - 1)$ internal vertices. Each leaf corresponds to an initial particle, each internal vertex corresponds to a merger of two clusters, and the edge lengths represent times between the respective mergers. The action of \mathcal{S}_t on such a tree coincides with a conditional aggregation process state that only considers clusters of mass $\geq t$. A well-studied special case is a coalescent process with a kernel $K(i, j)$, where all particles appear at instant $t = 0$ and each pair of clusters with masses i, j merges with intensity proportional to $K(i, j) = K(j, i)$, independently of all other pairs.

2.3. Relation to other generalizations of pruning. After completing the initial stage of this work, we have learned that a pruning operation similar in spirit to our generalized dynamical pruning (defined in Subsection 2.2) was considered in a preprint by Duquesne and Winkel [10] that extended a formalism by Evans [15] and Evans et al. [16]. We notice that the two definitions of pruning, ours in Subsection 2.2 and that in [10], are principally different, despite their similar appearance. In essence, the work [10] assumes the Borel measurability with respect to the Gromov-Hausdorff metric ([10], Section 2), which implies the semigroup property of the respective pruning ([10], Lemma 3.11). On the contrary, the generalized dynamical pruning of this study may have the semigroup property only under very particular choices of $\varphi(T)$; see Examples 1 and 2 above. The majority of natural choices of $\varphi(T)$, including the tree length $\varphi(T) = \text{LENGTH}(T)$ (Example 3) or the number of leaves in a tree (Example 4), do not have the semigroup property, and hence are not covered by the pruning of [10]. The main application results of this work (Section 4) refer to the pruning by $\varphi(T) = \text{LENGTH}(T)$ that has no semigroup property.

Curiously, for the above two examples with no semigroup property, i.e., when $\varphi(T) = \text{LENGTH}(T)$ and when $\varphi(T)$ equals the number of leaves in T , the following discontinuity property holds with respect to the Gromov-Hausdorff metric d_{GH} defined in [15, 16, 10]. For any $\epsilon > 0$ and any $M > 0$, there exist trees T and T' in $\mathcal{L}_{\text{plane}}$ such that

$$|\varphi(T) - \varphi(T')| > M \quad \text{while} \quad d_{\text{GH}}(T, T') < \epsilon.$$

Indeed, if $\varphi(T) = \text{LENGTH}(T)$, we consider a tree T with the number of leaves exceeding M/ϵ , and let T' be the tree obtained from T by elongating each of its leaves by ϵ . Similarly, if $\varphi(T)$ is the number of

leaves in T , we construct T' from T by attaching at least M/ϵ new leaves, each of length ϵ .

2.4. Invariance with respect to generalized dynamical pruning. Consider a tree $T \in \mathcal{L}_{\text{plane}}$ with edge lengths given by a positive vector $l_T = (l_1, \dots, l_{\#T})$. The edge length vector l_T can be specified by distribution $\chi(\cdot)$ of a point $x_T = (x_1, \dots, x_{\#T})$ on the standard simplex

$$\Delta^{\#T} = \left\{ x_i : \sum_i^{\#T} x_i = 1, 0 < x_i \leq 1 \right\},$$

and conditional distribution $F(\cdot | x_T)$ of the tree length $\text{LENGTH}(T)$, so that

$$l_T = x_T \times \text{LENGTH}(T).$$

Accordingly, a tree T can be completely specified by its planar shape, a vector of proportional edge lengths, and the total tree length:

$$T = \{\text{P-SHAPE}(T), x_T, \text{LENGTH}(T)\}.$$

A measure η on $\mathcal{L}_{\text{plane}}$ is a joint distribution of these three components:

$$\eta(T \in \{\tau, d\bar{x}, d\ell\}) = \mu(\tau) \times \chi_\tau(d\bar{x}) \times F_{\tau, \bar{x}}(d\ell),$$

where the tree planar shape is specified by

$$\mu(\tau) = \mathbf{Law}(\text{P-SHAPE}(T) = \tau), \quad \tau \in \mathcal{T}_{\text{plane}},$$

the relative edge lengths is specified by

$$\chi_\tau(\bar{x}) = \mathbf{Law}(x_T = \bar{x} | \text{P-SHAPE}(T) = \tau), \quad \bar{x} \in \Delta^{\#T},$$

and the total tree length is specified by

$$F_{\tau, \bar{x}}(\ell) = \mathbf{Law}(\text{LENGTH}(T) = \ell | x_T = \bar{x}, \text{P-SHAPE}(T) = \tau), \quad \ell \geq 0.$$

Let us fix $t \geq 0$ and a function $\varphi : \mathcal{L}_{\text{plane}} \rightarrow \mathbb{R}$ that is monotone non decreasing with respect to the partial order \leq . We denote by $\mathcal{S}_t^{-1}(\varphi, T)$ the preimage of a tree $T \in \mathcal{L}_{\text{plane}}$ under the generalized dynamical pruning:

$$\mathcal{S}_t^{-1}(\varphi, T) = \{\tau \in \mathcal{L}_{\text{plane}} : \mathcal{S}_t(\varphi, \tau) = T\}.$$

Consider the distribution of edge lengths induced by the pruning:

$$\Xi_\tau(\bar{x}) = \mathbf{Law}(x_{\tilde{T}} = \bar{x} | \text{P-SHAPE}(\tilde{T}) = \tau)$$

and

$$\Phi_{\tau, \bar{x}}(\ell) = \mathbf{Law}(\text{LENGTH}(\tilde{T}) = \ell | x_{\tilde{T}} = \bar{x}, \text{P-SHAPE}(\tilde{T}) = \tau),$$

where the notation $\tilde{T} := \mathcal{S}_t(\varphi, T)$ is used for brevity.

Definition 1 (Prune invariance). *Let fix $t \geq 0$ and a function $\varphi : \mathcal{L}_{\text{plane}} \rightarrow \mathbb{R}^+$ that is monotone non decreasing with respect to the partial order \leq . We call a measure η on $\mathcal{L}_{\text{plane}}$ invariant with respect to pruning $\mathcal{S}_t(\varphi, \cdot)$ (or simply prune invariant) if the following conditions hold*

- (i) *The measure is prune invariant in planar shapes. This means that for $\nu = \mu \circ \mathcal{S}_t^{-1}(\varphi, \cdot)$ we have*

$$\mu(\tau) = \nu(\tau | \tau \neq \phi).$$

- (ii) *The measure is prune invariant in edge lengths. This means that for any combinatorial planar tree $\tau \in \mathcal{T}_{\text{plane}}$*

$$\Xi_\tau(\bar{x}) = \chi_\tau(\bar{x})$$

and there exists a scaling exponent $\zeta \equiv \zeta(\varphi, t) > 0$ such that for any relative edge length vector $\bar{x} \in \Delta^{\#\tau}$ we have

$$\Phi_{\tau, \bar{x}}(\ell) = \zeta^{-1} F_{\tau, \bar{x}} \left(\frac{\ell}{\zeta} \right).$$

This definition unifies multiple invariance properties examined in the literature. For example, the classical work by Neveu [29] establishes prune invariance of critical Galton-Watson trees with i.i.d. exponential edge lengths with respect to tree erasure from leaves at a unit rate, which is equivalent to the generalized dynamical pruning with function $\varphi(T) = \text{HEIGHT}(T)$ (see Example 1). Prune invariance with respect to the Horton pruning (see Example 2 and Fig. 5) has been established by Burd et al. [9] for the combinatorial binary critical Galton-Watson trees with no edge lengths. Duquesne and Winkel [10] established prune-invariance of critical Galton-Watson trees with i.i.d. exponential edge lengths with respect to so-called *hereditary property*, which includes the tree erasure of Example 1 and Horton pruning of Example 2. The authors recently introduced a one-parameter family of *critical Tokunaga trees* [26] that are prune invariant with respect to the Horton pruning; this model includes the critical binary Galton-Watson tree with i.i.d. exponential lengths as a special case. Section 3.5 below establishes prune invariance of critical binary Galton-Watson trees with i.i.d. exponential edge lengths with respect to arbitrary generalized pruning.

3. DYNAMICAL PRUNING FOR EXPONENTIAL CRITICAL GALTON-WATSON TREES

We review here the results on tree representation of continuous functions, following [28, 30, 33, 36, 26].

3.1. **Harris path.** The *Harris path* of a tree $T \in \mathcal{L}_{\text{plane}}$ is defined as a piece-wise linear function [20, 33]

$$H_T(t) : [0, 2 \cdot \text{LENGTH}(T)] \rightarrow \mathbb{R}$$

that equals the distance from the root traveled along the tree T in the depth-first search, as illustrated in Fig. 7. For a tree T with n leaves, the Harris path $H_T(t)$ is a piece-wise linear positive excursion that consists of $2n$ linear segments with alternating slopes ± 1 , see [33].

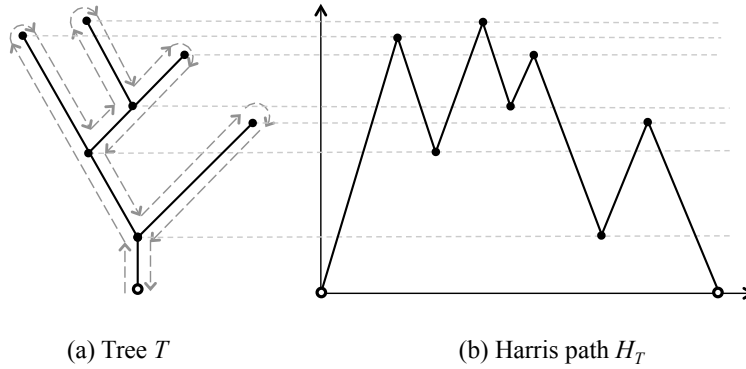


FIGURE 7. (a) Tree T and its depth-first search illustrated by dashed arrows. (b) Harris path $H_T(t)$ for the tree T of panel (a).

3.2. **Level set tree.** Consider a continuous function X_t , $t \in [a, b]$ with a finite number of local minima. The level set $\mathcal{L}_\alpha(X_t)$ is defined as the pre-image of the function values above α :

$$\mathcal{L}_\alpha(X_t) = \{t : X_t \geq \alpha\}.$$

The level set \mathcal{L}_α for each α is a union of non-overlapping intervals; we write $|\mathcal{L}_\alpha|$ for their number. Notice that $|\mathcal{L}_\alpha| = |\mathcal{L}_\beta|$ as soon as the interval $[\alpha, \beta]$ does not contain a value of local extrema of X_t ; and $0 \leq |\mathcal{L}_\alpha| \leq n$, where n is the number of the local maxima of X_t . As the threshold α decreases, the new intervals appear and the existing intervals merge. The *level set tree* $\text{LEVEL}(X_t) \in \mathcal{L}_{\text{plane}}$ is a tree that describes the topology of the level sets \mathcal{L}_α as a function of threshold α , as illustrated in Fig. 8.

Next we formally specify the combinatorial and metric structure of the level set tree, as well as its planar embedding.

Combinatorial structure of $\text{LEVEL}(X_t)$. Assume that there exist n local maxima of X_t , including possible local maxima at the boundaries of the interval $[a, b]$. Then there exist $(n - 1)$ internal minima, excluding possible local minima at the boundaries. Denote by

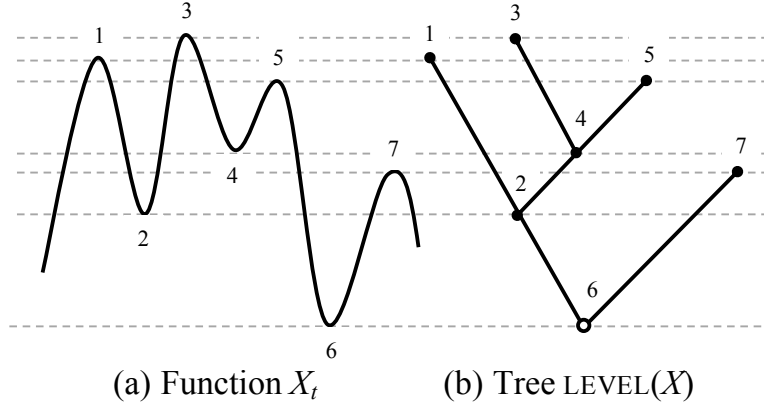


FIGURE 8. Function X_t (panel a) with a finite number of local extrema and its level-set tree $\text{LEVEL}(X)$ (panel b). The local extrema of X_t and the respective vertices of $\text{LEVEL}(X_t)$ are labelled by numbers 1 to 7. Local maxima (odd numbers) correspond to leaves, and local minima (even numbers) correspond to internal vertices of $\text{LEVEL}(X_t)$. The global minimum of X_t coincides with one of the internal local minima (label 6), so the level set tree is unplanted (root has degree 2).

$t_1 < t_2 < \dots < t_{2n-1}$ the ordered times of these local extrema. The level set tree $\text{LEVEL}(X_t)$ has $2n - 1$ vertices: n leaves that correspond (one-to-one) to the local maxima of X_t , and $n^{\text{int}} \leq n - 1$ non-root internal vertices that correspond (one-to-one) to the *chains* of equally-valued local minima of X_t . Formally, we say that two consecutive local minima at t_i and t_{i+2} belong to the same chain if $X_{t_i} = X_{t_{i+2}}$.

The tree root corresponds to the global minimum of X_t on $[a, b]$. If the global minimum is reached at the boundary ($t = a$ or $t = b$), then the root has degree 1 and the level set tree is planted; in this case the vertex that corresponds to the lowest local minimum within (a, b) is connected to the root. Otherwise, when the global minimum coincides with one of the local minima, the root corresponds to that local minimum, it has degree 2 and the level set tree is unplanted. This situation is illustrated in Fig. 8.

For every vertex i , except the one that corresponds to the lowest internal minimum of X_t and was discussed above, the parental vertex $\text{parent}(i)$ corresponds to the maximal of the two local minima adjacent to and below X_{t_i} . Formally, let s_j , $1 \leq j \leq n - 1$, denote the times of local minima within (a, b) . For every local extrema i , except the

lowest internal minimum, we define its right and left lower adjacent local minima:

$$r_i = \min_{1 \leq j \leq n-1} \{s_j : s_j > t_i \text{ and } X_{s_j} < X_{t_i}\},$$

$$l_i = \max_{1 \leq j \leq n-1} \{s_j : s_j < t_i \text{ and } X_{s_j} < X_{t_i}\}.$$

It is understood that one of r_i, l_i can be empty. In particular, $r_i = \emptyset$ for the rightmost internal minimum, $l_i = \emptyset$ for the leftmost internal minimum of X_t . We write $j \in \text{chain}(k)$ to denote that local minimum at s_j belongs to chain k for some $1 \leq k \leq n^{\text{int}}$. We now define

$$\text{parent}(i) = \{k : s_j = \arg \max(X_{r_i}, X_{l_i}) \text{ and } j \in \text{chain}(k)\},$$

with a convention that $X_\emptyset = \emptyset$ and $\max(a, \emptyset) = a$ for any $a \in \mathbb{R}$.

The chains of equally-valued local minima correspond to non-binary trees: the degree of a vertex that corresponds to a chain that includes k local minima is $k + 1$. The functions with distinct values of local minima correspond to binary trees.

Metric structure of $\text{LEVEL}(X_t)$. We specify the metric structure by assigning the edge lengths

$$|e_i| \equiv l_i = |X_{t_i} - X_{t_{\text{parent}(i)}}|$$

to all edges e_i .

Planar embedding of $\text{LEVEL}(X_t)$. The planar embedding (ordering) of the offspring of the same parent vertex coincides with that of the time instants t_i of the respective local extrema of X_t .

By construction, the level-set tree $\text{LEVEL}(X_t)$ is completely determined by the sequence of the values of local extrema of X_t . In particular, if $g(t)$ is a continuous and monotone increasing function on $[a, b]$, then the time transformation of X_t by function $g(t)$ does not disturb the level set tree:

$$\text{LEVEL}(X_t) = \text{LEVEL}(X_{g(t)}).$$

Hence, without loss of generality we can focus on the level set trees of continuous functions with alternating slopes ± 1 . To ensure that the level set tree of a function is binary, we need to eliminate the chains of equally-valued minima. This, for instance, is achieved if the distribution of lengths of linear segments has no atoms. We denote by \mathcal{E}^{ex} the space of finite piece-wise linear positive continuous excursions with alternating slopes ± 1 , atomless segment length distribution, and a finite number of segments.

By construction, the level set tree and Harris path are reciprocal to each other as described in the following statement.

Lemma 1 (Reciprocity of Harris path and level set tree). *The Harris path $H : \mathcal{L}_{\text{plane}}^{\downarrow} \rightarrow \mathcal{E}^{\text{ex}}$ and the level set tree $\text{LEVEL} : \mathcal{E}^{\text{ex}} \rightarrow \mathcal{L}_{\text{plane}}^{\downarrow}$ are reciprocal to each other. This means that for any $T \in \mathcal{L}_{\text{plane}}^{\downarrow}$ we have $\text{LEVEL}(H_T(t)) \equiv T$, and for any $Y_t \in \mathcal{E}^{\text{ex}}$ we have $H_{\text{LEVEL}(Y_t)}(t) \equiv Y_t$.*

3.3. Exponential critical binary Galton-Watson tree $\text{GW}(\lambda)$. Recall that a (combinatorial) critical binary Galton-Watson tree $T \in \mathcal{T}$ describes a trajectory of the Galton-Watson branching process. The process starts with a single progenitor (tree root) at time $t = 0$. At each discrete time step every existing population member terminates and produces, equiprobably, either no or two offspring, independently of the other members. We denote the resulting tree distribution on \mathcal{T} by $\mathcal{GW}^{\text{crit}}$.

Definition 2 (Exponential critical binary Galton-Watson tree).

We say that a random tree $T \in \mathcal{L}_{\text{plane}}^{\downarrow}$ is an exponential critical binary Galton-Watson tree with parameter $\lambda > 0$, and write $T \stackrel{d}{=} \text{GW}(\lambda)$, if

- (i) *SHAPE(T) is a critical binary Galton-Watson tree $\mathcal{GW}^{\text{crit}}$,*
- (ii) *the orientation for every pair of siblings in T is random and symmetric (e.g., in each pair of siblings, a randomly and uniformly selected sibling is assigned a right orientation, and the other is assigned a left orientation)*
- (iii) *given SHAPE(T), the edges of T are sampled as independent exponential random variables with parameter λ , i.e., with density*

$$(5) \quad \phi_{\lambda}(x) = \lambda e^{-\lambda x} \mathbf{1}_{\{x \geq 0\}}.$$

The following result is well-known.

Theorem 1. [33, Lemma 7.3],[28, 30] *Consider a random excursion $X_t \in \mathcal{E}^{\text{ex}}$. The level set tree $\text{LEVEL}(X_t)$ is an exponential critical binary Galton-Watson tree $\text{GW}(\lambda)$ if and only if the rises and falls of X_t , excluding the last fall, are distributed as independent exponential random variables with parameter $\lambda/2$.*

Consider a random walk $\{X_k\}_{k \in \mathbb{Z}}$ with a homogeneous transition kernel $p(x, y) \equiv p(x-y)$, for any $x, y \in \mathbb{R}$, given by a mixture of exponential jumps (Laplace distribution):

$$(6) \quad p(x) = \frac{\phi_{\lambda}(x) + \phi_{\lambda}(-x)}{2} = \frac{\lambda}{2} e^{-\lambda|x|}, \quad -\infty < x < \infty.$$

This process is called a *symmetric exponential random walk* with parameter λ . Each symmetric exponential random walk with parameter λ corresponds to a piece-wise linear continuous function $\{X_t\}_{t \in \mathbb{R}}$ with

slopes ± 1 whose alternating rises and falls, taken from $\{X_k\}_{k \in \mathbb{Z}}$, have independent exponential lengths with parameter $\lambda/2$. Specifically, consider a piece-wise linear function that interpolates the local extrema of X_k ; then transform the time in such a way that the slopes of the linear interpolation are ± 1 . There is one-to-one correspondence between the infinite sequences of the values of local extrema of $\{X_t\}_{t \in \mathbb{R}}$ and $\{X_k\}_{k \in \mathbb{Z}}$. We refer to such a function as a symmetric exponential random walk with parameter $\lambda/2$ on \mathbb{R} .

Corollary 1. *The Harris path $H_{\text{GW}(\lambda)}$ of an exponential critical binary Galton-Watson tree with parameter λ is an excursion of a symmetric exponential random walk $\{X_t\}_{t \in \mathbb{R}}$ with parameter $\lambda/2$.*

3.4. Length of a random tree $\text{GW}(\lambda)$. Recall the modified Bessel functions of the first kind

$$I_\nu(z) = \sum_{n=0}^{\infty} \frac{\left(\frac{z}{2}\right)^{2n+\nu}}{\Gamma(n+1+\nu)n!}.$$

Lemma 2. *Suppose $T \stackrel{d}{=} \text{GW}(\lambda)$ is an exponential critical binary Galton-Watson tree with parameter λ . The total length of the tree T has the probability density function*

$$(7) \quad \ell(x) = \frac{1}{x} e^{-\lambda x} I_1(\lambda x), \quad x > 0.$$

Proof. The number of different combinatorial shapes of a planar binary tree with $n+1$ leaves, and therefore $2n+1$ edges, is given by the *Catalan number* $C_n = \frac{1}{n+1} \binom{2n}{n} = \frac{(2n)!}{(n+1)!n!}$. The total length of $2n+1$ edges is a gamma random variable with parameters λ and $2n+1$ and density function

$$\gamma_{\lambda, 2n+1}(x) = \frac{\lambda^{2n+1} x^{2n} e^{-\lambda x}}{\Gamma(2n+1)}, \quad x > 0.$$

Hence, the total length of the tree T has the probability density function

$$(8) \quad \begin{aligned} \ell(x) &= \sum_{n=0}^{\infty} \frac{C_n}{2^{2n+1}} \cdot \frac{\lambda^{2n+1} x^{2n} e^{-\lambda x}}{(2n)!} = \sum_{n=0}^{\infty} \frac{\lambda^{2n+1} x^{2n} e^{-\lambda x}}{2^{2n+1} (n+1)! n!} \\ &= \frac{1}{x} e^{-\lambda x} \sum_{n=0}^{\infty} \frac{\left(\frac{\lambda x}{2}\right)^{2n+1}}{\Gamma(n+2) n!} = \frac{1}{x} e^{-\lambda x} I_1(\lambda x). \end{aligned}$$

□

Next, we compute the Laplace transform of $\ell(x)$. By the summation formula in (8),

$$\begin{aligned}\mathcal{L}\ell(s) &= \int_0^\infty \sum_{n=0}^\infty \frac{C_n}{2^{2n+1}} \cdot \frac{\lambda^{2n+1} x^{2n} e^{-(\lambda+s)x}}{(2n)!} dx \\ &= \sum_{n=0}^\infty \frac{C_n}{2^{2n+1}} \cdot \left(\frac{\lambda}{\lambda+s}\right)^{2n+1} \int_0^\infty \frac{(\lambda+s)^{2n+1} x^{2n} e^{-(\lambda+s)x}}{(2n)!} dx \\ &= \sum_{n=0}^\infty \frac{C_n}{2^{2n+1}} \cdot \left(\frac{\lambda}{\lambda+s}\right)^{2n+1} = Z \cdot c(Z^2),\end{aligned}$$

where we let $Z = \frac{\lambda}{2(\lambda+s)}$, and the characteristic function of Catalan numbers

$$c(z) = \sum_{n=0}^\infty C_n z^n = \frac{2}{1 + \sqrt{1 - 4z}}$$

is well known. Therefore

$$(9) \quad \mathcal{L}\ell(s) = Z \cdot c(Z^2) = \frac{\lambda}{\lambda + s + \sqrt{(\lambda + s)^2 - \lambda^2}}.$$

Note that the Laplace transform $\mathcal{L}\ell(s)$ could be derived from the total probability formula

$$(10) \quad \ell(x) = \frac{1}{2}\phi_\lambda(x) + \frac{1}{2}\phi_\lambda * \ell * \ell(x),$$

where $\phi_\lambda(x)$ is the exponential p.d.f. (5). Thus, $\mathcal{L}\ell(s)$ solves

$$(11) \quad \mathcal{L}\ell(s) = \frac{1}{2} \frac{\lambda}{\lambda + s} \left(1 + (\mathcal{L}\ell(s))^2\right).$$

Corollary 2. *The probability density function $f(x)$ of the length of an excursion in an exponential symmetric random walk with parameter λ is given by*

$$(12) \quad f(x) = \frac{1}{2}\ell(x/2).$$

Proof. Observe that the excursion has twice the length of a tree $\text{GW}(\lambda)$. \square

3.5. **Prune invariance of $\text{GW}(\lambda)$.** This section establishes prune invariance of exponential Galton-Watson trees with respect to arbitrary generalized pruning.

Theorem 2. *Let $T \stackrel{d}{=} \text{GW}(\lambda)$ be an exponential critical binary Galton-Watson tree with parameter $\lambda > 0$. Then, for any monotone non-decreasing function $\varphi : \mathcal{L}_{\text{plane}} \rightarrow \mathbb{R}^+$ and any $\Delta > 0$ we have*

$$T^\Delta := \{\mathcal{S}_\Delta(\varphi, T) | \mathcal{S}_\Delta(\varphi, T) \neq \phi\} \stackrel{d}{=} \text{GW}(\lambda p_\Delta(\lambda, \varphi)),$$

where $p_\Delta(\lambda, \varphi) = \mathbb{P}(\mathcal{S}_\Delta(\varphi, T) \neq \phi)$. That is, the pruned tree T^Δ conditioned on surviving is an exponential critical binary Galton-Watson tree with parameter

$$\mathcal{E}_\Delta(\lambda, \varphi) = \lambda p_\Delta(\lambda, \varphi).$$

Proof. Let X denote the length of the edge of T adjacent to the root of T , and let Y denote the length of the edge of T^Δ adjacent to the root of T^Δ . Let x be the descendent vertex (a junction or a leaf) to the root in T . Then X , which is an exponential random variable with parameter λ , represents the distance from the root of T to x . Let $\text{deg}_T(x)$ denote the degree of x in tree T and $\text{deg}_{T^\Delta}(x)$ denote the degree of x in tree T^Δ . If $T^\Delta = \phi$, then $Y = 0$. Let

$$F(h) = \mathbb{P}(Y \leq h | \mathcal{S}_\Delta(\varphi, T) \neq \phi).$$

The event $\{Y \leq h\}$ is partitioned into the following non-overlapping sub-events S_1, \dots, S_4 illustrated in Fig. 9:

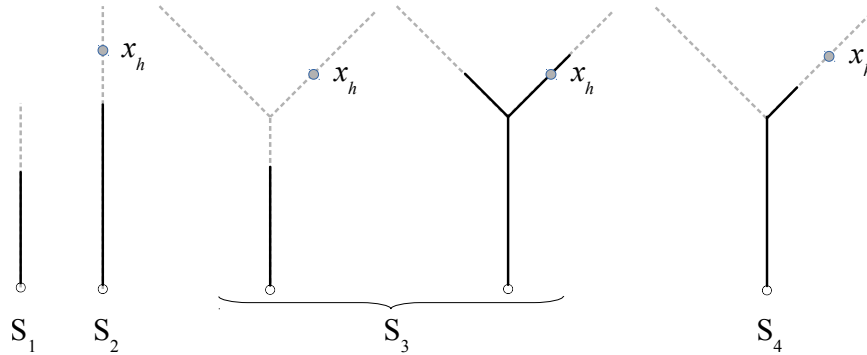


FIGURE 9. Sub-events used in the proof of Theorem 2. Gray dashed line shows (a part of) initial tree T . Solid black line shows (a part of) pruned tree T^Δ . We denote by x_h a point in T located at distance h from the root, if it exists.

(S₁) The event $\{\deg_T(x) = 1 \text{ and } X \leq h\}$ has probability

$$\frac{1}{2}(1 - e^{-\lambda h}).$$

(S₂) The event $\{X > h \text{ and all points of } T \text{ descendant to } x_h \text{ do not belong to } T^\Delta\}$ has probability

$$e^{-\lambda h}(1 - p_\Delta).$$

(S₃) The event $\{X \leq h \text{ and } \deg_T(x) = 3 \text{ and either both subtrees of } T \text{ descending from } x \text{ are pruned away completely (not intersecting } T^\Delta) \text{ or } \{x \in T^\Delta, \deg_{T^\Delta}(x) = 3\}\}$ has probability

$$\frac{1}{2}(1 - e^{-\lambda h})((1 - p_\Delta)^2 + p_\Delta^2).$$

(S₄) The event $\{\{X \leq h, \deg_T(x) = 3\} \text{ and } \{x \in T^\Delta, \deg_{T^\Delta}(x) = 2\} \text{ and } Y \leq h\}$ has probability¹

$$\frac{1}{2} \int_0^h \lambda e^{-\lambda t} \cdot 2p_\Delta(1 - p_\Delta) \cdot F(h - t) dt = p_\Delta(1 - p_\Delta) \int_0^\infty \lambda e^{-\lambda t} F(h - t) dt.$$

Using this we have two representations for the probability $P(Y \leq h)$:

$$\begin{aligned} P(Y \leq h) &= (1 - p_\Delta) + p_\Delta F(h) \\ &= \frac{1}{2}(1 - e^{-\lambda h}) + e^{-\lambda h}(1 - p_\Delta) \\ &\quad + \frac{1}{2}(1 - e^{-\lambda h})((1 - p_\Delta)^2 + p_\Delta^2) \\ &\quad + p_\Delta(1 - p_\Delta) \int_0^\infty \lambda e^{-\lambda t} F(h - t) dt, \end{aligned}$$

which simplifies to

$$(1 - p_\Delta) + p_\Delta F(h) = (1 - p_\Delta + p_\Delta^2) - e^{-\lambda h} p_\Delta + p_\Delta(1 - p_\Delta) \int_0^\infty \lambda e^{-\lambda t} F(h - t) dt.$$

Differentiating the above equality we obtain the following equation for the probability density function $f(y) = \frac{d}{dy} F(y)$ of Y :

$$f(h) = p_\Delta \phi_\lambda(h) + (1 - p_\Delta) \phi_\lambda * f(h),$$

¹Here, $\deg_{T^\Delta}(x) = 2$ means x is neither a junction nor a leaf in T^Δ .

where as before ϕ_λ denotes the exponential density with parameter λ . Applying integral transformation on both sides of the equation, we obtain the characteristic function $\hat{f}(s) = E[e^{isY}]$ of Y ,

$$\hat{f}(s) = \frac{\lambda p_\Delta}{\lambda p_\Delta - is} = \hat{\phi}_{\lambda p_\Delta}(s).$$

Thus, we conclude that Y is an exponential random variable with parameter λp_Δ .

Next, let y be the descendent vertex (a junction or a leaf) to the root in T^Δ . If $T^\Delta = \phi$, let y denote the root. Let

$$q = \mathbf{P}(\mathbf{deg}_{T^\Delta}(y) = 3 \mid \mathcal{S}_\Delta(T) \neq \phi).$$

Then,

$$\begin{aligned} p_\Delta q &= \mathbf{P}(\mathbf{deg}_{T^\Delta}(y) = 3) \\ &= \mathbf{P}(\mathbf{deg}_T(x) = 3) \cdot \left\{ \mathbf{P}(\mathbf{deg}_{T^\Delta}(x) = 3 \mid \mathbf{deg}_T(x) = 3) \right. \\ &\quad \left. + \mathbf{P}(\mathbf{deg}_{T^\Delta}(x) = 2 \mid \mathbf{deg}_T(x) = 3) \cdot q \right\} \\ &= \frac{1}{2} \left\{ p_\Delta^2 + 2p_\Delta(1 - p_\Delta)q \right\} \end{aligned}$$

implying

$$q = \frac{1}{2}p_\Delta + (1 - p_\Delta)q,$$

which in turn yields $q = \frac{1}{2}$.

We saw that conditioning on $\mathcal{S}_\Delta(\varphi, T) \neq \phi$, the pruned tree T^Δ has the edge connecting the root to its descendent vertex y distributed exponentially with parameter λp_Δ . Then, with probability $q = \frac{1}{2}$, the pruned tree T^Δ branches at y into two independent subtrees, each distributed as $\{T^\Delta \mid T^\Delta \neq \phi\}$. Thus, we recursively obtain that T^Δ is a critical binary Galton-Watson tree with i.i.d. exponential edge length with parameter λp_Δ . \square

Next, we find an exact form of the survival probability $p_\Delta(\lambda, \varphi)$ for three particular choices of φ , thus obtaining $\mathcal{E}_\Delta(\lambda, \varphi)$.

Theorem 3. *In the settings of Theorem 2, we have*

(a): *If $\varphi(T)$ equals the total length of T ($\varphi = \text{LENGTH}(T)$), then*

$$\mathcal{E}_\Delta(\lambda, \varphi) = \lambda e^{-\lambda\Delta} \left[I_0(\lambda\Delta) + I_1(\lambda\Delta) \right].$$

(b): If $\varphi(T)$ equals the height of T ($\varphi = \text{HEIGHT}(T)$), then

$$\mathcal{E}_\Delta(\lambda, \varphi) = \frac{2\lambda}{\lambda\Delta + 2}.$$

(c): If $\varphi(T) + 1$ equals the Horton-Strahler order of the tree T , then

$$\mathcal{E}_\Delta(\lambda, \varphi) = \lambda 2^{-\lfloor \Delta \rfloor},$$

where $\lfloor \Delta \rfloor$ denotes the maximal integer $\leq \Delta$.

Proof. Part (a). By Lemma 2,

$$\begin{aligned} p_\Delta &= 1 - \int_0^\Delta \ell(x) dx = 1 - \int_0^{\lambda\Delta} \frac{1}{x} e^{-x} I_1(x) dx \\ (13) \quad &= e^{-\lambda\Delta} \left[I_0(\lambda\Delta) + I_1(\lambda\Delta) \right], \end{aligned}$$

where for the last equality we used formula 11.3.14 in [2].

Part (b). Using the representation of an exponential critical binary Galton-Watson tree $\text{GW}(\lambda)$ via its Harris path as in Theorem 1, we consider a symmetric exponential random walk Y_k with jump distribution given by (6), and notice that Y_k is a martingale.

The probability p_Δ now can be interpreted for the Harris path as the probability that a given excursion of Y_k is above Δ for some k . This would guarantee that the depth of a tree exceeds Δ . Specifically, let $T_0 = \min\{k > 1 : Y_k \leq 0\}$. We condition on $Y_1 > 0$, and consider an excursion Y_0, Y_1, \dots, Y_{T_0} . Here

$$p_\Delta = \mathbf{P} \left(\max_{j: 0 < j < T_0} Y_j > \Delta \mid Y_1 > 0 \right).$$

The problem of finding p_Δ is solved using the Optional Stopping Theorem. Let

$$T_\Delta = \min\{k > 0 : Y_k \geq \Delta\} \quad \text{and} \quad T := T_\Delta \wedge T_0.$$

Next, observe that

$$p_\Delta = \mathbf{P}(T = T_\Delta \mid Y_1 > 0).$$

For a fixed $y \in (0, \Delta)$, by the Optional Stopping Theorem, we have

$$\begin{aligned}
y &= E[Y_T \mid Y_1 = y] \\
&= E[Y_T \mid T = T_0, Y_1 = y]P(T = T_0 \mid Y_1 = y) \\
&\quad + E[Y_T \mid T = T_\Delta, Y_1 = y]P(T = T_\Delta \mid Y_1 = y) \\
&= E[Y_T \mid Y_T \leq 0, Y_1 = y]P(T = T_0 \mid Y_1 = y) \\
&\quad + E[Y_T \mid Y_T \geq \Delta, Y_1 = y]P(T = T_\Delta \mid Y_1 = y) \\
&= -\frac{1}{\lambda}P(T = T_0 \mid Y_1 = y) + \left(\Delta + \frac{1}{\lambda}\right)P(T = T_\Delta \mid Y_1 = y) \\
&= \left(\Delta + \frac{2}{\lambda}\right)P(T = T_\Delta \mid Y_1 = y) - \frac{1}{\lambda}.
\end{aligned}$$

Hence,

$$P(T = T_\Delta \mid Y_1 = y) = \frac{y + \frac{1}{\lambda}}{\Delta + \frac{2}{\lambda}}.$$

Thus,

$$\begin{aligned}
P\left(T = T_\Delta, 0 < Y_1 < \Delta \mid Y_1 > 0\right) &= \int_0^\Delta P(T = T_\Delta \mid Y_1 = y) \lambda e^{-\lambda y} dy \\
&= \int_0^\Delta \frac{y + \frac{1}{\lambda}}{\Delta + \frac{2}{\lambda}} \lambda e^{-\lambda y} dy \\
&= \frac{2}{\lambda\Delta + 2} - e^{-\lambda\Delta},
\end{aligned}$$

and therefore,

$$\begin{aligned}
p_\Delta &= P\left(\max_{j: 0 < j < K} Y_j > \Delta \mid Y_1 > 0\right) \\
&= P\left(T = T_\Delta, 0 < Y_1 < \Delta \mid Y_1 > 0\right) + P\left(T = T_\Delta, Y_1 \geq \Delta \mid Y_1 > 0\right) \\
&= \frac{2}{\lambda\Delta + 2} - e^{-\lambda\Delta} + P\left(Y_1 \geq \Delta \mid Y_1 > 0\right) \\
&= \frac{2}{\lambda\Delta + 2}.
\end{aligned}$$

Part (c). Follows from [26, Corollary 1]. \square

Remark 1. Let $\mathcal{E}_\Delta(\lambda, \varphi) = \frac{2\lambda}{\lambda\Delta + 2}$ as in Theorem 3(b). Here $\mathcal{E}_0\lambda = \lambda$ and $\mathcal{E}_\Delta(\lambda, \varphi)$ is a linear-fractional transformation associated with

matrix

$$\mathcal{A}_\Delta = \begin{pmatrix} 1 & 0 \\ \frac{\Delta}{2} & 1 \end{pmatrix}.$$

Since \mathcal{A}_Δ form a subgroup in $SL_2(\mathbb{R})$, the transformations $\{\mathcal{E}_\Delta\}_{\Delta \geq 0}$ satisfy the semigroup property

$$\mathcal{E}_{\Delta_1} \mathcal{E}_{\Delta_2} = \mathcal{E}_{\Delta_1 + \Delta_2}$$

for any pair $\Delta_1, \Delta_2 \geq 0$.

We notice also that the operator $\mathcal{E}_\Delta(\lambda, \varphi)$ in part (c) of Theorem 3 satisfies only the discrete semigroup property for nonnegative integer times. Finally, one can check that $\mathcal{E}_\Delta(\lambda, \varphi)$ in part (a) does not satisfy the semigroup property.

4. CONTINUUM BALLISTIC ANNIHILATION MODEL, $A + A \rightarrow \emptyset$

Here we turn to the dynamics of particles governed by 1-D ballistic annihilation model. Section 4.1 introduces the model and describes the natural emergence of sinks (shocks). The model initial conditions are given by a particle velocity distribution and particle density on \mathbb{R} . We consider here a constant density and initial velocity distribution with alternating values ± 1 , or, equivalently, initial piece-wise linear potential $\psi(x, 0)$ with alternating slopes ± 1 (Fig. 2). Section 4.2 summarizes the basic constraints on the model dynamics. Section 4.3 provides a construction of the shock tree (Lemma 5) and its graphical embedding into the phase space $(x, \psi(x, t))$ and space-time domain (x, t) . Theorem 4 states that the shock tree is the level set tree for the initial potential $\psi(x, 0)$. Theorem 5 in Section 4.4 establishes equivalence of the ballistic annihilation dynamics and a generalized dynamical pruning of a mass-equipped shock tree.

4.1. Continuum model, sinks, and shock trees. The ballistic annihilation model describes the dynamics of a set of particles that move with given initial velocities and annihilate at collision, hence the model notation $A + A \rightarrow \emptyset$ [13, 5, 7, 32, 12, 6, 14, 8, 27, 34]. The model dynamics is illustrated in Fig. 1. We introduce here a continuum mechanics formulation of ballistic annihilation, analyzing the dynamics of a mass distributed on the real line. This formulation makes sense when a large number of particles densely populates the system.

Formally, we are given a Lebesgue measurable initial density $g(x) \geq 0$ of particles on a line \mathbb{R} . The initial particle velocities are given by $v(x, 0) = v(x)$. Prior to collision and subsequent annihilation, a particle

located at x_0 at time $t = 0$ moves according to its initial velocity, so its coordinate $x(t)$ changes as

$$(14) \quad x(t) = x_0 + tv(x_0).$$

When the particle collides with another particle, it annihilates. Accordingly, two particles with initial coordinates and velocities (x_-, v_-) and (x_+, v_+) collide and annihilate at time t when they meet at the same new position,

$$x_- + tv_- = x_+ + tv_+,$$

given that neither of the particles annihilated prior to t . In this case the annihilation time is given by

$$(15) \quad t = -\frac{x_+ - x_-}{v_+ - v_-}.$$

Let $v(x, t)$ be the Eulerian specification of the velocity field at coordinate x and time instant t ; we define the corresponding *potential function*

$$\psi(x, t) = -\int_a^x v(y, t)dy,$$

so that $v(x, t) = -\partial_x \psi(x, t)$. Let $\psi(x, 0) = \Psi_0(x)$ be the initial potential.

We call a point $\sigma(t)$ *sink* (or *shock*), if there exist two particles that annihilate at coordinate s at time t . Suppose $v(x) \in \mathcal{C}^1(\mathbb{R})$. The equation (15) implies that appearance of a sink is associated with a negative local minima of $v'(x^*)$ such that there exists a neighborhood of x^* contained in the support of $g(x)$; we call such points *sink sources*. Specifically, if x^* is a sink source, then a sink will appear at time $t^* = -1/v'(x^*)$ and location given by

$$\sigma(t^*) = x^* + t^*v(x^*) = x^* - \frac{v(x^*)}{v'(x^*)}$$

unless the particle with initial coordinate x^* annihilated before time t^* .

Sinks, which originate at sink sources, can move and coalesce (see Fig. 1). We refer to a sink trajectory as a *shock wave*. We impose the conservation of mass condition by defining the *mass of a sink* at time t to be the total mass of particles annihilated in the sink between time zero and time t . When sinks coalesce, their masses add up. It will be convenient to assume that sinks do not disappear when they stop accumulating mass. Informally, we assume that the sinks are being pushed by the system particles. Formally, there exists several cases depending on the occupancy of a neighborhood of $\sigma(t)$. If there

exists an empty neighborhood around the sink coordinate $\sigma(t)$, the sink is considered at rest (its coordinate does not change). If only the left neighborhood of $\sigma(t)$ is empty, and the right adjacent velocity is negative:

$$v(\sigma_+, t) := \lim_{x \downarrow \sigma(t)} v(x, t) < 0,$$

the sink at $\sigma(t)$ moves with velocity $v(\sigma_+, t)$. A similar rule is applied to the case of right empty neighborhood. The appearance, motion, and subsequent coalescence of sinks can be described by a time oriented *shock tree*. In particular, the coalescence of sinks under initial conditions with a finite number of sink sources is described by a finite tree.

The dynamics of ballistic annihilation, either in discrete or continuum versions, can be quite intricate and is lacking a general description. The existing analyses focus on the evolution of selected statistics under particular initial conditions. In the next section, we outline some basic principles that can facilitate the analysis of the continuum ballistic annihilation. We then give a complete description of the dynamics in case of two-valued initial velocity and constant particle density. Specifically, we describe the evolution of a constant-slope potential $\psi(t, x)$ within a finite spatial domain for $t > 0$.

4.2. Basic constraints on ballistic annihilation dynamics. Suppose $x_- < x_+$ are such that $v(x_-) > v(x_+)$. Assume that density $g(x)$ is positive, and suppose there is only one sink source $x^* \in (x_-, x_+)$. In order for x_- and x_+ to annihilate each other in the sink originated at x^* at time $t > t^*$ we need the following:

(i) Collision at time t :

$$x_- + tv(x_-) = x_+ + tv(x_+).$$

(ii) The mass between x_- and x^* annihilates the mass between x^* and x_+ :

$$\int_{x_-}^{x^*} g(x) dx = \int_{x^*}^{x_+} g(x) dx.$$

(iii) Neither x_- nor x_+ is annihilated before time t .

From conditions (i) and (ii), we obtain the location of the sink at time t :

$$(16) \quad \sigma(t) = \frac{v(x_-) \frac{g(x_-)}{1+tv'(x_-)} + v(x_+) \frac{g(x_+)}{1+tv'(x_+)}}{\frac{g(x_-)}{1+tv'(x_-)} + \frac{g(x_+)}{1+tv'(x_+)}}.$$

This sink dynamics description is not restricted to $v(x) \in \mathcal{C}^1(\mathbb{R})$, and can be extended to the case of piecewise smooth $v(x)$.

Example 5 (Two velocities, single sink). Suppose $g(x)$ is positive.

Let $v(x) = \begin{cases} v_- & \text{if } x \leq x^* \\ v_+ & \text{if } x > x^* \end{cases}$, where the constants $v_- > v_+$ and x^* are

given. Naturally, x^* is the only sink source and the only sink appears at the sink source at time $t = 0$. Moreover, analogously to (16), one can derive the dynamics of the sink at time t :

$$(17) \quad \sigma(t) = \frac{v_- g(x_-) + v_+ g(x_+)}{g(x_-) + g(x_+)},$$

where $x_- < x^*$ is the only root of $G_t(y) = \int_{x^*}^{y+t(v_- - v_+)} g(x) dx - \int_y^{x^*} g(x) dx$, and $x_+ = x_- + t(v_- - v_+)$. Note that $G_t(x)$ is continuous and strictly increasing, and that $G_t(x^*) > 0 > G_t(x^* - t(v_- - v_+))$.

4.3. Piece-wise linear potential with unit slopes. The discrete 1-D ballistic annihilation model with two possible velocities $\pm v$ was considered in [13, 7, 6, 14, 8]; the three velocity case ($-1, 0$, and $+1$) appeared in [12, 34]. We study a continuum version of the 1-D ballistic annihilation with two possible initial velocities and constant initial density, i.e. $v(x) = \pm v$ and $g(x) \equiv g_0$. Since we can scale both space and time, without loss of generality we let $v(x) = \pm 1$ and $g(x) \equiv 1$. More formally, we consider an initial potential $\psi(x, 0) = \Psi_0(x)$ that is a negative piece-wise linear excursion on a finite interval with segment slopes ± 1 ; see Fig. 2. We denote the space of such functions $\widetilde{\mathcal{E}}^{\text{ex}}$, and write $\widetilde{\mathcal{E}}^{\text{ex}}([a, b])$ if the domain $[a, b] \subset \mathbb{R}$ is explicitly given. This space bears a lot of symmetries that facilitate our analysis.

Observe that the domain $[a, b]$ is partitioned into non-overlapping subintervals with boundaries x_j such that the initial particle velocity assumes alternating values of ± 1 within each interval, with boundary values $v(a, 0) = 1$ and $v(b, 0) = -1$. For a finite interval $[a, b]$, there exists a finite time $t_{\text{max}} = (b - a)/2$ at which all particles aggregate into a single sink of mass $m = (b - a)$; see discussion below. We only consider the solution on the time interval $[0, t_{\text{max}}]$, and assume that the density of particles vanishes outside of $[a, b]$.

Since we assumed a unit mass density, the model dynamics is completely determined by the potential $\Psi_0(x)$. The trajectories of the sinks in this model have a tree structure; we denote the respective shock tree by $S(\Psi_0)$.

Our first goal is to construct the system trajectory, including the trajectories of the massive sinks, in the phase space

$$(x, \psi(x, t)) \in \mathbb{R}^2, x \in [a, b], t \in [0, (b - a)/2]$$

and in the respective space-time domain (x, t) . We do this below for consecutively more complicated potentials. We focus on the shock wave tree $S(\Psi_0)$, and demonstrate that this tree can be used to reconstruct the entire system dynamics.

V-shaped potential. Let $x_1 = c = (a + b)/2$ be the center of the segment $[a, b]$. Consider a simplest V-shaped potential that consists of a negative segment on $[a, c]$ and a positive segment on $[c, b]$, see Fig. 10. In this case, there exists a single sink that originates at $t = 0$ at the point $(c, \Psi_0(c))$. In x -space, it remains at rest and accumulates mass at rate 2 during the time interval of duration $(b - a)/2$, which reflects accumulation of particles that merge into the sink from left and right. After this, the mass of the sink is $(b - a)$, which reflects complete accumulation of mass from the interval $[a, b]$.

In the phase space (Fig. 10, bottom panel), the trajectory of the sink corresponds to a vertical segment of length $v_1 = (b - a)/2$ between points $(x_1, \Psi_0(x_1))$ and $(x_1, \Psi_0(x_1) + v_1)$. The trajectory of each particle is a horizontal line from the particle's initial position $(x, \psi(x, 0))$ to the point of merging with the sink at $(x_1, \psi(x, 0))$.

In the space-time domain (Fig. 10, top panel) the trajectory of the sink is a vertical segment between points $(x_1, 0)$ and (x_1, v_1) . The trajectories of particles, each of which moves with its initial velocity until merging with the sink, is shown by thin diagonal lines.

W-shaped potential. Consider now a negative excursion on $[a, b]$ with exactly two local minima at x_1, x_3 and the only local maxima at x_2 , with $a < x_1 < x_2 < x_3 < b$, see Fig. 11. There exist two sinks that originate at $t = 0$ at points x_1 and x_3 . The sink at x_1 remains at rest and accumulates mass at rate 2 during time interval of duration $v_1 = \Psi_0(x_2) - \Psi_0(x_1)$. At instant $t = v_1$ the right neighborhood of the sink at x_1 becomes empty, and it starts moving at unit speed to the right. Similarly, the sink at x_3 remains at rest and accumulates mass at rate 2 during time interval of duration $v_3 = \Psi_0(x_2) - \Psi_0(x_3)$. At instant $t = v_3$ the left neighborhood of the sink at x_3 becomes empty, and it starts moving at unit speed to the left. The two sinks move toward each other until they merge to form a new sink of mass $2(v_1 + v_3)$. We denote by $h_i, i = 1, 3$ the durations of these respective movements. Since both right and left neighborhoods of the new sink are occupied by regular particles, the particle remains at rest for some time.

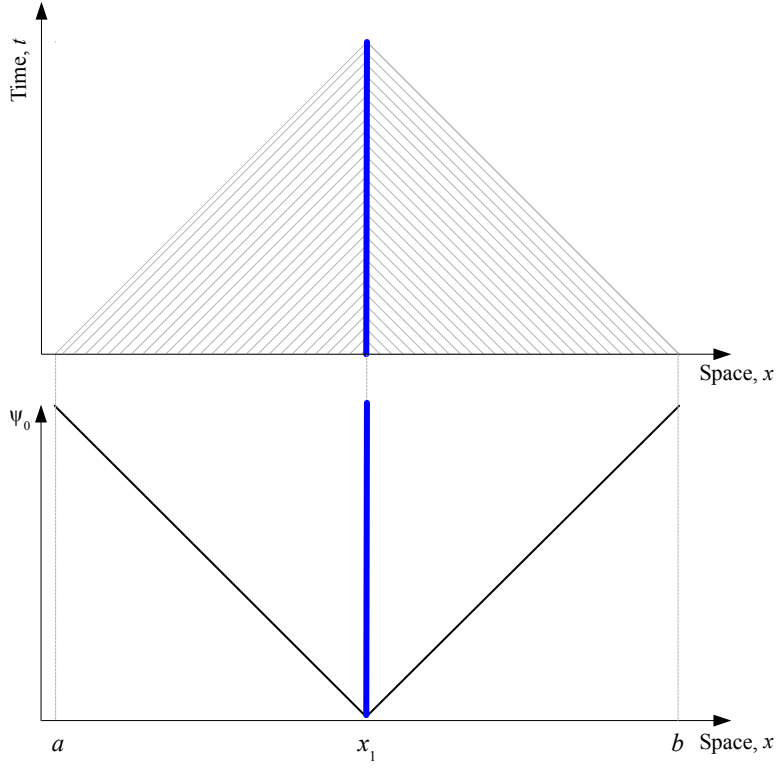


FIGURE 10. A V-shaped potential. (Bottom): The potential Ψ_0 (black line) and the shock wave in the phase space (x, ψ) (blue segment). (Top): The space-time portrait. The system occupies a triangular (shaded) region in the (x, t) space. Thin hatching illustrates the trajectories of particles. Blue vertical segment show the trajectory of the sink.

The following lemma describes the shape of the respective graphical shock trees $\mathcal{G}^{(x,\psi)}(\Psi_0)$ and $\mathcal{G}^{(x,t)}(\Psi_0)$ in the phase space and space-time domain, respectively.

Lemma 3 (Shock tree of a W-shaped potential). *For a W-shaped potential described above (and illustrated in Fig. 11) we have:*

- (a) *The graphical shock tree $\mathcal{G}^{(x,\psi)}(\Psi_0)$ in the phase space has the bracket shape that consists of two leaves and a root edge (Fig. 11, bottom panel). Each leaf corresponds to the dynamics of one of the two initial sinks; the root edge corresponds to the dynamics of the final sink. Each leaf consists of a vertical segment between points $(x_i, \Psi_0(x_i))$ and $(x_i, \Psi_0(x_2))$, and a horizontal segment between points $(x_i, \Psi_0(x_2))$ and $(c, \Psi_0(x_2))$, for $i = 1, 3$. The*

stem consists of a vertical segment between points $(c, \Psi_0(x_2))$ and $(c, \Psi_0(a))$. Here $c = (a + b)/2$ is the center of the interval $[a, b]$.

- (b) In the space-time domain (x, t) , the system occupies a cone \mathcal{C} that has the shape of a right triangle with the hypotenuse on the interval $x \times t = [a, b] \times \{0\}$ and the catheti merging at the point (c, c) . The trajectories of the sinks form an inverted Y-shaped tree shown in Fig. 11 (top panel) that consists of two leaves and a stem. Each leaf corresponds to the dynamics of one of the two initial sinks; the stem corresponds to the dynamics of the final sink. Each leaf consists of a vertical segment between points $(x_i, 0)$ and (x_i, v_i) , and a slanted segment between points (x_i, v_i) and $(c, v_1 + v_3)$, for $i = 1, 3$. The stem consists of a vertical segment between points $(c, v_1 + v_3)$ and (c, c) . There exists a rectangular empty region (no particles) with vertices at the points (clock-wise from the bottom point): $(x_2, 0)$, (x_1, v_1) , $(c, v_1 + v_3)$, and (x_3, v_3) .
- (c) The particles move with their initial velocities until they merge with a sink. A particle x in the interval $[x_1 - v_1, x_1 + v_1 = x_2]$ merges with the sink at point x_1 at time instant $t = |x_1 - x|$. A particle x in the interval $(x_3 - v_3 = x_2, x_3 + v_3]$ merges with the sink at point x_3 at time instant $t = |x_3 - x|$. A particle x in the intervals $[a, x_1 - v_1)$ and $(x_3 + v_3, b]$ merges with the sink at point $(a + b)/2$ at time instant $t = |(a + b)/2 - x|$. The particle at x_2 merges the sink at x_1 (x_3) if the potential is left (right) continuous at time instant $t = x_2 - x_1$ ($t = x_3 - x_2$).

Proof. By construction of the solution of the continuum annihilation dynamics for a potential $\Psi_0(x) \in \widetilde{\mathcal{E}}^{\text{ex}}([a, b])$, see Fig. 11. \square

We make now an important symmetry observation, which helps to extend our geometric construction of the shock tree to an arbitrary potential from $\widetilde{\mathcal{E}}^{\text{ex}}$. We define the *basin* \mathcal{B}_j for a local maximum at x_j as the shortest interval that contains x_j and supports a non-positive excursion in $\Psi_0(x)$. Formally, $\mathcal{B}_j = [x_j^{\text{left}}, x_j^{\text{right}}]$, where

$$x_j^{\text{right}} = \inf(x : x > x_j \text{ and } \Psi_0(x) > \Psi(x_j)),$$

$$x_j^{\text{left}} = \sup(x : x < x_j \text{ and } \Psi_0(x) > \Psi(x_j)).$$

The basin length is denoted by $|\mathcal{B}_j| = x_j^{\text{right}} - x_j^{\text{left}}$.

Lemma 4 (Symmetry lemma). *Let v_i, h_i for $i = 1, 3$ be the lengths of the vertical and horizontal segments, respectively, of the leaves of the*

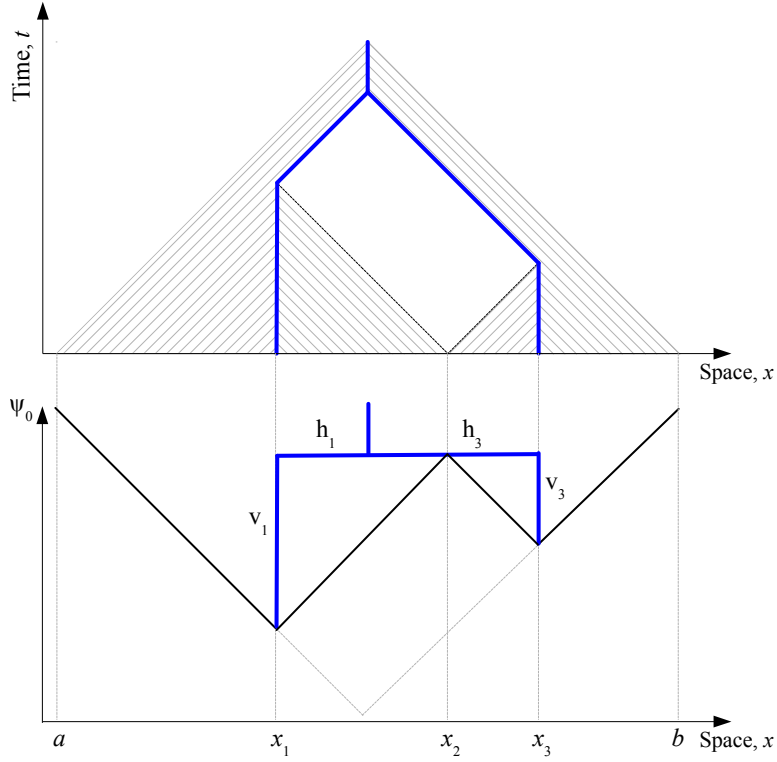


FIGURE 11. A W-shaped potential. (Bottom): The potential Ψ_0 (solid black) and the shock in the phase space (x, ψ) (blue). (Top): The space-time portrait. The system occupies a shaded region in the (x, t) space, bounded by a triangle that corresponds to the V-shaped potential on the interval $[a, b]$, as in Fig. 10. Notice the appearance of an empty rectangular region in the space-time portrait that corresponds to (x, t) locations with no particles. Thin hatching illustrates the trajectories of particles. Blue lines show the trajectories of sinks.

shock tree for a W-shaped potential (see Fig. 11):

$$v_i = \Psi_0(x_2) - \Psi_0(x_i), \quad h_i = |(a+b)/2 - x_i|.$$

Then

$$h_1 = v_3, \quad h_3 = v_1$$

and

$$v_i + h_i = |\mathcal{B}_2|/2 = (b-a)/2 - (\Psi_0(a) - \Psi_0(x_2)).$$

Proof. By elementary geometric properties of the tree for a W-shaped potential illustrated in Fig. 11. \square

Lemma 4 implies that after instant $t = |\mathcal{B}_2|/2$ when the sinks that originate at x_1 and x_3 merge, the process dynamics is indistinguishable from that of the V-shaped potential on $[a, b]$. This allows us to construct the shock tree in a general case, using a sequential construction by basin lengths.

General potential. Consider a potential $\Psi_0(x) \equiv \Psi_1(x) \in \widetilde{\mathcal{E}}^{\text{ex}}([a, b])$. The shock tree for the V-shaped potential was constructed above. If the potential is not V-shaped, it has $n \geq 1$ local maxima (see illustrations in Figs. 12,13). Consider the basins that correspond to the local maxima of $\Psi_1(x)$ and index them according to their lengths, from shortest to longest:

$$|\mathcal{B}_1| < |\mathcal{B}_2| < \cdots < |\mathcal{B}_n|.$$

Let $t_i = |\mathcal{B}_i|/2$. For each basin \mathcal{B}_i we define the corresponding *space-time cone* \mathcal{C}_i that has the shape of a right triangle with hypotenuse $x \times t = \mathcal{B}_i \times \{0\}$ and the catheti merging at the point $(x_i^{\text{left}} + t_i, t_i)$.

It is readily seen that the shortest basin necessarily corresponds to a W-shaped potential. We construct the shock tree for the regular particles within the space interval \mathcal{B}_1 during the time interval $[0, t_1]$, using the W-shaped potential construction of Lemma 3. Hence, we describe the system dynamics in the space-time cone \mathcal{C}_1 .

Consider now an *unfolded* potential $\Psi_2(x)$ that coincides with $\Psi_1(x)$ outside of \mathcal{B}_1 and has a V-shaped form on \mathcal{B}_1 . By construction, and using Lemma 3, the trees that correspond to the potentials Ψ_1 and Ψ_2 coincide outside of the cone \mathcal{C}_1 in the space-time domain. The potential $\Psi_2(x)$ has $n - 1$ local minima. Its shortest basin is \mathcal{B}_2 ; it necessarily corresponds to a W-shaped potential within $\Psi_2(x)$. We use $\Psi_2(x)$ to construct the space-time tree on \mathcal{C}_2 , using the W-shaped potential algorithm of Lemma 3. The resulting tree is only considered within the space-time subregion $\mathcal{C}_2 \setminus \mathcal{C}_1$. The union of this tree and the tree constructed in the initial step within \mathcal{C}_1 results in the tree within $\mathcal{C}_1 \cup \mathcal{C}_2$.

Consider now a set of unfolded potentials $\Psi_i(x)$, $i = 3, \dots, n$, such that $\Psi_i(x)$ coincides with $\Psi_{i-1}(x)$ on $[a, b] \setminus \mathcal{B}_i$ and has a V-shaped negative excursion on \mathcal{B}_{i-1} , see Fig. 12. By construction, the shortest basin within every $\Psi_i(x)$ is \mathcal{B}_i ; and this basin supports a W-shaped potential. We apply the W-shaped potential algorithm to each potential $\Psi_i(x)$ within the basin \mathcal{B}_i , hence consecutively extending the shock tree construction to the space-time subsets

$$\bigcup_{j=1}^i \mathcal{C}_j, \quad i = 3, \dots, n.$$

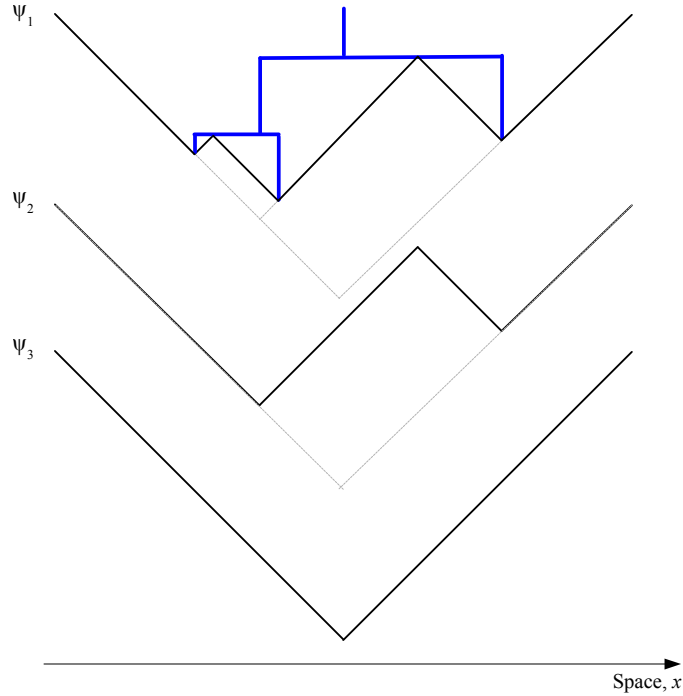


FIGURE 12. Potential unfolding: an illustration. The potential $\Psi_2(x)$ is an unfolding of $\Psi_1(x)$, and $\Psi_3(x)$ is an unfolding of $\Psi_2(x)$. The shock tree in the phase space is shown (blue segments) next to the initial potential $\Psi_1(x)$.

At instant t_n there exists a single sink within a V-shaped potential $\Psi_n(x)$ on $[a, b]$, which is treated according to the V-shaped potential construction. This completes the space-time tree construction.

Figure 13 illustrates the above process for a potential with 4 local maxima. The space-time cones \mathcal{C}_i , $i = 1, \dots, 5$ are labeled in the figure. Here, the largest cone \mathcal{C}_5 corresponds to the entire space-time system's domain.

Observe that the graphical shock trees $\mathcal{G}^{(x,\psi)}$ and $\mathcal{G}^{(x,t)}$ in the phase space and in the space-time domain have the same combinatorial structure and planar embedding, coinciding with that of $S(\Psi_0)$ (recall that embedding only involves ordering between the offspring of the same parent, and is different from a particular graphical representation of a tree); see Figs. 10,11,14.

Combinatorial tree structure and planar embedding. By construction, there is one-to-one correspondence between internal local maxima of $\Psi_0(x)$ and internal non-root vertices of $S(\Psi_0)$. There is also a one-to-one correspondence between local minima and the leaves. We

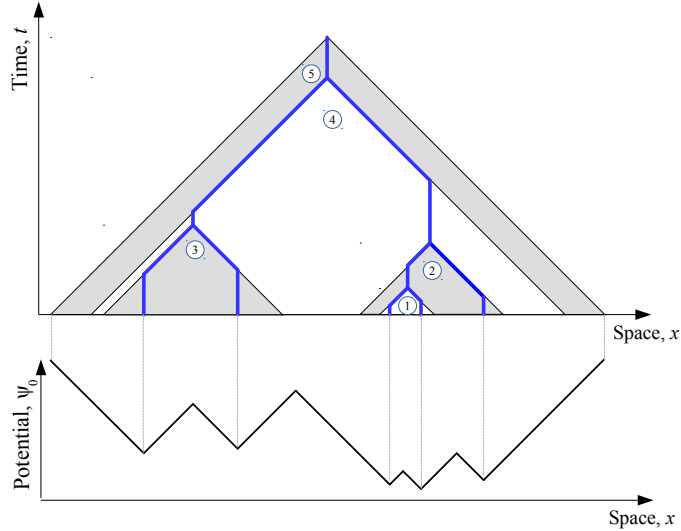


FIGURE 13. Iterative solution construction: an illustration for a potential $\Psi_0(x)$ (bottom panel) with four local maxima. (Top): Space-time cones $\mathcal{C}_1, \dots, \mathcal{C}_4$ that correspond to the basins $\mathcal{B}_1, \dots, \mathcal{B}_4$. Blue segments show the shock tree. The cone \mathcal{C}_5 corresponds to the V-shaped potential on the whole space interval.

label the tree vertices by indices j that correspond to the local extrema x_j of $\Psi_0(x)$.

Each internal non-root vertex j has degree 2. To find its offspring, consider the basin \mathcal{B}_j of a local maximum x_j . It is sub-divided into two sub-basins by point x_j . The right (left) offspring of j corresponds to the internal local extrema with the maximal value within the right (left) sub-basin. In case of a V-shaped potential, this is the only local minimum. Otherwise, it is the internal local maximum with the maximal value.

We write $\text{parent}(i)$ for the index of the single parent of the vertex i ; $\text{right}(i)$ and $\text{left}(i)$ for the indices of the right and left offspring of an internal non-root vertex i ; and $\text{sibling}(i)$ for the index of the sibling of vertex i .

Metric tree structure in the phase space. We let c_i be the center of the basin \mathcal{B}_i and

$$v_i = \Psi_0(x_{\text{parent}(i)}) - \Psi_0(x_i), \quad h_i = |\mathcal{B}_{\text{sibling}(i)}|/2.$$

The length l_i of the parental edge of a non-root vertex i within $S(\Psi_0)$ is given by $l_i = v_i + h_i$. The shock tree $S(\Psi_0)$ can be considered a length metric space with the Euclidean length measured along the tree

branches. Figure 14 shows graphical shock trees $\mathcal{G}^{(x,\psi)}$ and $\mathcal{G}^{(x,t)}$ for an initial potential with two local maxima and three local minima and illustrates the labeling of vertical (v_i) and horizontal (h_i) segments of the tree.

Graphical shock tree in the phase space. Here we give a concise description of the graphical tree $\mathcal{G}^{(x,\psi)}(\Psi_0)$, which is the union of the following vertical and horizontal segments:

- (v_{\min}) For every local minimum x_j there exists a vertical segment from $(x_j, \Psi_0(x_j))$ to $(x_j, \Psi_0(x_j) + v_j)$.
- (v_{\max}) For every local maximum x_j there exists a vertical segment from $(c_j, \Psi_0(x_j))$ to $(c_j, \Psi_0(x_j) + v_j)$.
- (h) For every local maximum x_j there exists a horizontal segment of length h_j from $(c_{\text{left}(j)}, \Psi_0(x_j))$ to $(c_{\text{right}(j)}, \Psi_0(x_j))$.

The following statement summarizes the correspondence between the dynamics of the sinks and the graphical tree $\mathcal{G}^{(x,\psi)}(\Psi_0)$. An analogous statement holds for the graphical shock tree $\mathcal{G}^{(x,t)}(\Psi_0)$ in the space-time domain.

Lemma 5 (Shock tree). *Let $\mathcal{G} \equiv \mathcal{G}^{(x,\psi)}(\Psi_0)$ be the graphical shock tree of a continuum annihilation dynamics with potential $\Psi_0(x) \in \widetilde{\mathcal{E}}^{\text{ex}}([a, b])$. The following statements hold:*

- a) *There exists a one-to-one correspondence between points $z \in \mathcal{G}$ and space-time locations (x_z, t_z) of sinks. In particular, there exists a one-to-one correspondence between the sinks at instant $t = 0$ and the leaves of \mathcal{G} , and a one-to-one correspondence between the instants when two sink merge (and hence a new sink creates) and the internal vertices of \mathcal{G} .*
- b) *Every sink at any time can either be at rest and accumulate mass at rate 2, or move with a unit speed with no mass accumulation. A point on any vertical segment of \mathcal{G} corresponds to a sink at rest. A point on any horizontal segment of \mathcal{G} corresponds to a sink in motion.*
- c) *Suppose a point $z \in \mathcal{G}$ corresponds to a sink with mass m_z at location (x_z, t_z) . Then t_z equals the length from z to any descendant leaf within \mathcal{G} . The mass $m_z \leq 2t_z$ equals double the total length of the vertical part of the tree \mathcal{G} descendant to z . In particular, $m_z = 2t_z$ if and only if z is located on a vertical segment of \mathcal{G} .*
- d) *The horizontal segment of every vertex within \mathcal{G} has the length equal to the total length of the vertical segments within its sibling*

tree. In other words, the time spent by a sink in motion equals half the mass of the sink with which it collides.

Proof. Follows from the construction of the tree $\mathcal{G}^{(x,\psi)}(\Psi_0)$ and Lemmas 3,4. \square

Consider a tree $\mathcal{V}(\Psi_0) \in \mathcal{L}_{\text{plane}}$ that has the same combinatorial structure as $S(\Psi_0)$, and with edge lengths given by $l_i = v_i$. Informally, this is a tree that consists of the vertical segments of the graphical tree $\mathcal{G}^{(x,\psi)}(\Psi_0)$.

Theorem 4 (Shock tree is a level set tree). *Consider a potential $\Psi_0(x) \in \widetilde{\mathcal{E}}^{\text{ex}}$ and the corresponding tree $\mathcal{V}(\Psi_0) \in \mathcal{L}_{\text{plane}}^{\dagger}$. Then the tree $\mathcal{V}(\Psi_0)$ is equivalent to the level set tree of the negative potential $-\Psi_0(x)$:*

$$\text{LEVEL}(-\Psi_0) = \mathcal{V}(\Psi_0).$$

Proof. Follows from construction of the shock trees and the level set tree. Considering a negative potential reflects the fact that the level set tree is constructed top to bottom (leaves correspond to local maxima), and the shock tree is constructed bottom to top (leaves correspond to local minima). \square

4.4. Ballistic annihilation of a unit-slope potential. Suppose that a tree $T \in \mathcal{L}_{\text{plane}}$ has a particular graphical representation $\mathcal{G}_T \in \mathbb{R}^2$ and let $f : T \rightarrow \mathcal{G}_T$ be a bijective root-preserving isometry. We define the generalized dynamical pruning $\mathcal{S}_t(\varphi, \mathcal{G}_T)$ for the graphical tree \mathcal{G}_T as the f -image of $\mathcal{S}_t(\varphi, T)$:

$$\mathcal{S}_t(\varphi, \mathcal{G}_T) = f[\mathcal{S}_t(\varphi, T)].$$

Consider a natural isometry between the graphical shock tree $\mathcal{G}^{(x,t)}(\Psi_0)$ in the space-time domain and tree $\mathcal{G}^{(x,\psi)}(\Psi_0)$ in the phase space or the shock tree $S(\Psi_0)$. By construction (and using the natural isometry), the ballistic annihilation dynamics of the sinks corresponds to the continuous pruning (erosion) of the shock tree $S(\Psi_0)$, or its graphical representations, from the leaves. Recall that this corresponds to selecting $\varphi(T) = \text{HEIGHT}(T)$ in the generalized dynamical pruning framework.

It is readily seen that the potential $\psi(x, t)$ at any given $t > 0$ can be uniquely reconstructed from either of the pruned graphical trees $\mathcal{G}^{(x,t)}(\Psi_0)$ and $\mathcal{G}^{(x,\psi)}(\Psi_0)$. Because of the strong symmetries (see Lemmas 4, 5d), the graphical trees possess significant redundant information. We show below that the reduced tree $\mathcal{V}(\Psi_0)$, equipped with information about the sinks provides a minimal description sufficient for reconstructing the entire continuum annihilation dynamics.

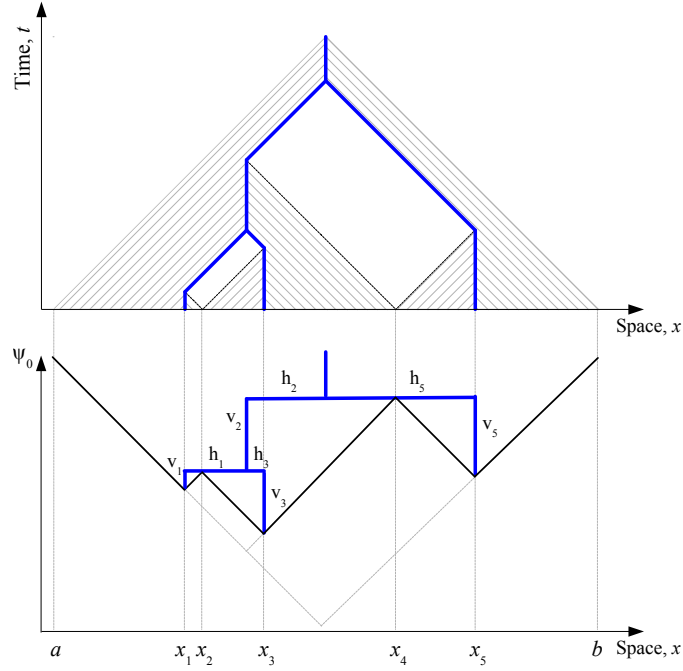


FIGURE 14. Shock tree for a piece-wise linear potential with two local maxima. (Top): The shock tree in space-time domain (blue). Hatching illustrates motion of regular particles. There exist two empty rectangular areas, each corresponding to one of the local maxima. (Bottom): Potential $\Psi_0(x)$ (black) and the shock tree in the phase space (blue). The figure illustrates the labeling of vertical (v_i) and horizontal (h_i) segments of the tree.

First, we expand the space $\mathcal{L}_{\text{plane}}$ by equipping the trees with oriented massive sinks. Specifically, consider a tree $T \in \mathcal{L}_{\text{plane}}$. A non-vertex point $z \in T$ can be equipped with an oriented mass $m_L > 0$ (left) or $m_R > 0$ (right). Every leaf vertex is necessarily equipped with either a single (un-oriented) mass $m \geq 0$, or a pair of positive masses (m_L, m_R) . Finally, we assume that that number of sinks within a tree is finite. The new space of mass-equipped trees is denoted by $\tilde{\mathcal{L}}_{\text{plane}}$. Observe that any tree $T \in \mathcal{L}_{\text{plane}}$ can be considered as an element of $\tilde{\mathcal{L}}_{\text{plane}}$ with no internal mass (no sinks attached to non-vertex points) and zero mass at the leaves.

Construction 1 (Potential \rightarrow tree). *Suppose that $\psi(x, 0) \in \tilde{\mathcal{E}}^{\text{ex}}$ and fix $t \in (0, t_{\text{max}}]$. A mass-equipped tree $T_\psi(t) \in \tilde{\mathcal{L}}_{\text{plane}}$ for the potential $\psi(x, t)$ is constructed as follows:*

- (a) *The planar shape of the tree, as an element of $\mathcal{L}_{\text{plane}}$, corresponds to the level set tree of the potential restricted to the positive density domain: $\psi(x, t)|_{g(x, t) > 0}$. (This corresponds, for any given $t > 0$, to cutting zero-density space intervals and glueing the potential segments from positive-density intervals to form a continuous function from $\widetilde{\mathcal{E}}^{\text{ex}}$.)*
- (b) *Every leaf that corresponds to a local minimum point of $\psi(x, t)$ is equipped with mass $m = 2t$.*
- (c) *Every leaf that corresponds to a local minimum plateau of length ε in $\psi(x, t)$ is equipped with an arbitrary double mass $(m_{\text{L}}, m_{\text{R}})$ that satisfies*

$$m_{\text{L}} + m_{\text{R}} = \varepsilon + 2t.$$

- (d) *Every internal point that corresponds to a plateau of length ε that is not a local maximum is equipped with mass $m = v$.*

Remark 2. The non-unique choices in item (c) reflect the memory loss of the ballistic annihilation dynamics.

Definition 3. A tree $T \in \widetilde{\mathcal{L}}_{\text{plane}}$ is called t -admissible for a given $t \geq 0$ if and only if its masses satisfy the following conditions:

- (a1) *Any internal mass m satisfies $m < 2t$.*
- (a2) *Any single mass m at a leaf satisfies $m = 2t$.*
- (a3) *Any mass pair $(m_{\text{L}}, m_{\text{R}})$ at a leaf satisfies $m_{\text{L}} + m_{\text{R}} > 2t$.*

For any t -admissible tree $T \in \widetilde{\mathcal{L}}_{\text{plane}}$ one can construct a unique corresponding potential $\psi_{T, t}(x)$.

Construction 2 (Tree \rightarrow potential). Suppose that $T \in \widetilde{\mathcal{L}}_{\text{plane}}$ is a t -admissible tree for some $t > 0$. The corresponding potential $\psi_{T, t}(x) \in \widetilde{\mathcal{E}}^{\text{ex}}$ is constructed in the following steps:

- (1) *Construct the Harris path $H_T(x)$ of T as an element of $\mathcal{L}_{\text{plane}}^{\downarrow}$.*
- (2) *At every local minimum of $H_T(x)$ that corresponds to a double mass $(m_{\text{L}}, m_{\text{R}})$, insert a horizontal plateau of length*

$$\varepsilon = m_{\text{L}} + m_{\text{R}} - 2t.$$

- (3) *At every monotone point of $H_T(x)$ that corresponds to an internal mass m , insert a horizontal plateau of length m .*
- (4) *At every local maxima, insert a horizontal plateau of length $2t$.*

We now extend the definition of the generalized dynamical pruning to the mass-equipped trees.

Definition 4 (Cuts). *The set $\mathcal{D}_t(\varphi, T)$ of cuts in a pruned tree $\mathcal{S}_t(\varphi, T)$ is defined as the boundary of the pruned part of the tree*

$$\mathcal{D}_t(\varphi, T) = \partial\{x \in T : \varphi(\Delta_{x,T}) < t\}.$$

Accordingly, the set of tree cuts is a union of the leaves of the pruned tree and the vertices of the initial tree that became edge points in the pruned tree.

Every cut point $z \in \mathcal{S}_t(\varphi, T)$ is equipped with either single or double mass. If the root of the subtree $\Delta_{z,T}$ has degree 1, the point z is equipped with mass m_z equal to the value of the pruning function φ at the subtree $\Delta_{z,T}$. If the root of the subtree $\Delta_{z,T}$ has degree 2, the subtree $\Delta_{z,T}$ is comprised of two subtrees, T_1 and T_2 , that merge (and share the root) at z . In this case, the point z is equipped with mass(es) equal to the value(s) of φ at every tree T_i such that $\varphi(T_i) < t$. We denote the mass-equipped generalized dynamical pruning by $\tilde{\mathcal{S}}_t(\varphi, T)$.

The following theorem establishes the equivalence of the continuum annihilation dynamics and mass-equipped generalized dynamical pruning with respect to the tree length.

Theorem 5 (Annihilation pruning). *Suppose that $\psi(x, 0) \in \tilde{\mathcal{E}}^{\text{ex}}$. For any fixed $t \geq 0$, let $T_\psi(t)$ be the mass-equipped tree for the potential $\psi(x, t)$. Then the following statements hold:*

- (a) *The tree $T_\psi(t)$ is t -admissible, and it uniquely reproduces the potential:*

$$\psi(x, t) = \psi_{T_\psi(t), t}(x).$$

- (b) *The ballistic annihilation dynamics of the potential $\psi(x, t)$ corresponds to a generalized mass-equipped dynamical pruning of the tree*

$$T_\psi(0) = \text{LEVEL}(\psi(x, 0)),$$

considered as an element of $\tilde{\mathcal{L}}_{\text{plane}}$, with $\varphi(T) = \text{LENGTH}(T)$:

$$T_\psi(t) = \tilde{\mathcal{S}}_t(\text{LENGTH}, T_\psi(0)).$$

Proof. We start by proving the statement for a W-shaped potential. Consider a W-shaped potential $\Psi_0(x)$ with two local minima at x_i , $i = 1, 3$ and the local maximum at x_2 (see Fig. 11). We define (as before) $v_i = \Psi_0(x_2) - \Psi_0(x_i)$ and set $v_{\min} = v_1 \wedge v_3$, $v_{\max} = v_1 \vee v_3$. There exist four stages in the ballistic annihilation dynamics of a W-shaped potential, illustrated in Fig. 15.

- 1:** During the time interval $t \in (0, v_{\min})$, there exist two sinks (at rest) located in the local minima of $\psi(x, t)$. This corresponds to

a Y-shaped tree $T_\psi(t)$ with no internal sinks and mass $m = 2t$ at each of the leaves.

- 2:** During the time interval $t \in [v_{\min}, v_{\max})$, there exist two sinks. One is at rest and is located in the (only) local minima of $\psi(x, t)$; and the other moves and is located next to a plateau. This corresponds to an I-shaped tree $T_\psi(t)$ with an internal mass $m_R = 2v_{\min}$ placed at distance $v_{\max} - t$ from the leaf and mass $m = 2t$ at the leaf.
- 3:** During the time interval $t \in [v_{\max}, v_1 + v_3)$, there exist two sinks in motion. They both are located at the boundaries of the plateau. This corresponds to an I-shaped tree $T_\psi(t)$ with no internal mass and a double mass $(2v_1, 2v_3)$ at the leaf.
- 4:** During the time interval $t \in [v_1 + v_3, t_{\max})$, there exists a single sink at rest. It is located at the local minimum of the potential. This corresponds to an I-shaped tree $T_\psi(t)$ with no internal mass and a single mass $m = 2t$ at the leaf.

The statements (a) and (b) for a W-shaped potential are verified by direct observation in each of the four stages, and using Constructions 1,2.

The general case is now treated by considering the nested W-shaped potentials via the unfolding procedure, as in the sequential cone-based construction of the solution to the continuum annihilation dynamics in Section 4.3. \square

5. BALLISTIC ANNIHILATION OF AN EXPONENTIAL EXCURSION

This section analyses a special case of a piece-wise linear potential with unit slopes: a negative exponential excursion. Consider potential $\psi(x, 0) = -H_{\text{GW}(\lambda)}(x)$ that is the negative Harris path of an exponential critical binary Galton-Watson tree with parameter λ . In words, the potential is a negative finite excursion with linear segments of alternating slopes ± 1 , such that the lengths of all segments except the last one are i.i.d. exponential random variables with parameter $\lambda/2$. This means that the initial particle velocity $v(x, 0)$ alternates between the values ± 1 at epochs of a stationary Poisson point process on \mathbb{R} with rate $\lambda/2$, starting with $+1$ and until the respective potential crosses the zero level.

Corollary 3 (Exponential excursion). *Let potential $\Psi_0(x) \in \widetilde{\mathcal{E}}^{\text{ex}}$ be a negative exponential excursion, $\Psi_0(x) = -H_{\text{GW}(\lambda)}(x)$. Then the corresponding shock tree $\mathcal{V}(\Psi_0) \in \mathcal{L}_{\text{plane}}^1$ is an exponential binary critical Galton-Watson tree $\text{GW}(\lambda)$.*

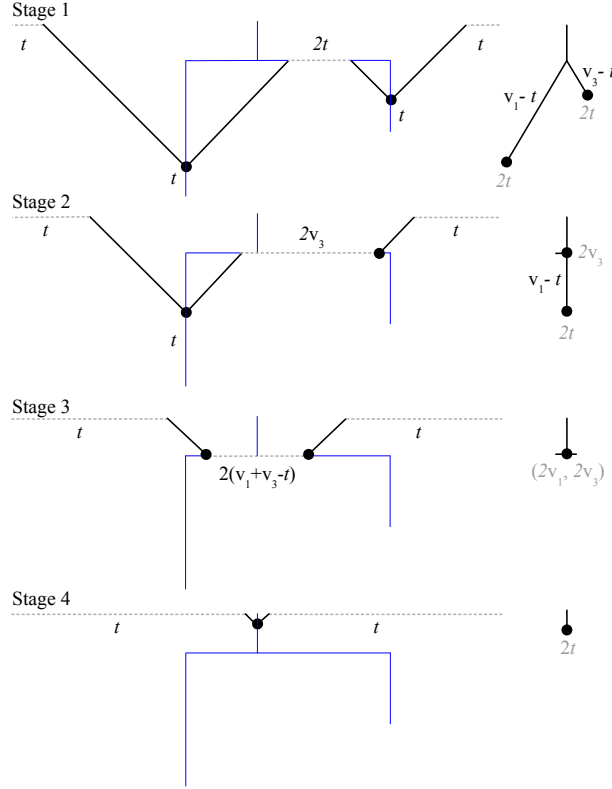


FIGURE 15. Four generic stages in the ballistic annihilation dynamics of a W-shaped potential (left), and respective mass-equipped trees (right). (Left): Potential (solid black) $\psi(x, t)$. Each plateau (dashed gray) corresponds to an empty interval. The graphical shock tree $\mathcal{G}^{(x, \phi)}(\Psi_0)$ (blue) and sinks (black circles) are shown for visual convenience. (Right): Mass-equipped trees. Segment lengths are marked in black, point masses are indicated in gray. A tick next to the mass point in Stage 2 indicates its orientation (left). A double-tick next to the mass point in Stage 3 indicates two masses at the leaf.

Proof. By Theorem 4, the shock tree $\mathcal{V}(\Psi_0)$ is the level set tree of the negative potential $-\Psi_0(x)$. The statement now follows from Theorem 1. \square

By Theorem 5 the ballistic annihilation dynamics of an initial potential $\psi(x, 0)$ is equivalent to a generalized dynamical pruning of the

respective mass-equipped tree $T_\psi(0)$ with pruning function $\varphi(T) = \text{LENGTH}(T)$. Here we give a complete description of the ballistic annihilation dynamics for a mass-equipped exponential critical binary Galton-Watson tree $T_\psi(t) \in \tilde{\mathcal{L}}_{\text{plane}}$.

Recall that if $T = \text{GW}(\lambda)$ and $\varphi(T) = \text{LENGTH}(T)$, then by (13),

$$p_t := \mathbf{P}(\varphi(T) > t) = e^{-\lambda t} \left[I_0(\lambda t) + I_1(\lambda t) \right].$$

Theorem 6 (Ballistic annihilation dynamics of an exponential excursion). *Suppose the initial potential $\psi(x, 0)$ is the negative Harris path of an exponential critical binary Galton-Watson tree with parameter λ , $T = T_\psi(0) \stackrel{d}{=} \text{GW}(\lambda)$. Then, at any instant $t > 0$ the mass-equipped shock tree $T_\psi(t) = \tilde{\mathcal{S}}_t(\text{LENGTH}, T_\psi(0))$ conditioned on surviving, $T_\psi(t) \neq \emptyset$, is distributed according to the following rules.*

- (i) $T_\psi(t) \stackrel{d}{=} \text{GW}(\lambda_t)$ with $\lambda_t := \lambda p_t$.
- (ii) A single or double mass points are placed independently in each leaf with the probability of a single mass being

$$\frac{2 \ell(t)}{\lambda p_t^2}.$$

- (iii) Each single mass at a leaf has mass $m = 2t$. For a double mass point, the masses (m_L, m_R) has the following joint p.d.f.

$$f(a, b) = \frac{\frac{1}{4} \ell(\frac{a}{2}) \ell(\frac{b}{2})}{p_t^2 - \frac{2}{\lambda} \ell(t)}$$

for $a, b > 0$, $a \vee b \leq 2t < a + b$.

- (iv) The number of mass points placed in the interior of any edge is distributed geometrically with the probability of placing k masses being

$$p_t (1 - p_t)^k, \quad k = 0, 1, 2, \dots$$

The locations of k mass points are independent uniform in the interior of the edge. The orientation of each mass is left or right independently with probability $1/2$.

- (v) The edge masses are i.i.d. random variables with the following common p.d.f.

$$\frac{\ell(\frac{a}{2})}{2(1 - p_t)}, \quad a \in (0, 2t).$$

Proof. Part (i) follows directly from Theorem 3(a).

To establish the other parts, we first introduce a particular representation of the survival event $\mathcal{S}_t(\varphi, T) \neq \emptyset$. Let X denote the length of

the edge of T adjacent to the root and let x be the descendent vertex (a junction or a leaf) to the root in T . If $\deg_T(x) = 3$, let h_1 and h_2 represent the lengths of the two subtrees descendent from x . Then the event $\mathcal{S}_t(\varphi, T) \neq \phi$ can be written as the union of the following five non-overlapping events, illustrated in Fig. 16,

$$\begin{aligned}
 \left\{ \mathcal{S}_t(\varphi, T) \neq \phi \right\} = & \{ \deg_T(x) = 3 \text{ and } t \leq h_1 \wedge h_2 \} \\
 & \cup \{ \deg_T(x) = 3 \text{ and } h_1 \wedge h_2 \leq t < h_1 \vee h_2 \} \\
 & \cup \{ \deg_T(x) = 3 \text{ and } h_1 \vee h_2 \leq t < h_1 + h_2 \} \\
 & \cup \{ \deg_T(x) = 3 \text{ and } h_1 + h_2 \leq t < X + h_1 + h_2 \} \\
 (18) \quad & \cup \{ \deg_T(x) = 1 \text{ and } t < X \}.
 \end{aligned}$$

The probabilities of the five events in (18) are computed below.

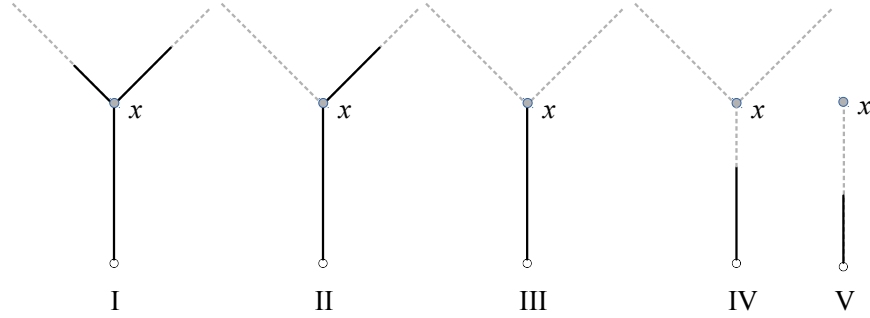


FIGURE 16. Subevents used in the proof of Theorem 6. Solid line depicts (a part of) pruned tree $\mathcal{S}_t(\varphi, T)$. Dashed line depicts (a part of) initial tree T .

Case I

$$\begin{aligned}
 \mathbb{P}(\deg_T(x) = 3 \text{ and } t \leq h_1 \wedge h_2) &= \frac{1}{2} \mathbb{P}(t \leq h_1 \wedge h_2 \mid \deg_T(x) = 3) \\
 (19) \quad &= \frac{p_t^2}{2}.
 \end{aligned}$$

Case II

$$\begin{aligned}
 \mathbb{P}(\deg_T(x) = 3 \text{ and } h_1 \wedge h_2 \leq t < h_1 \vee h_2) &= \frac{1}{2} \mathbb{P}(h_1 \wedge h_2 \leq t < h_1 \vee h_2 \mid \deg_T(x) = 3) \\
 &= \mathbb{P}(h_1 < h_2 \mid \deg_T(x) = 3) \\
 (20) \quad &= p_t(1 - p_t).
 \end{aligned}$$

Case III

$$\begin{aligned}
& \mathbf{P}(\deg_T(x) = 3 \text{ and } h_1 \vee h_2 \leq t < h_1 + h_2) \\
&= \frac{1}{2} \mathbf{P}(h_1 \vee h_2 \leq t < h_1 + h_2 \mid \deg_T(x) = 3) \\
&= \frac{1}{2} \mathbf{P}(h_1 \vee h_2 \leq t \mid \deg_T(x) = 3) - \frac{1}{2} \mathbf{P}(t < h_1 + h_2 \mid \deg_T(x) = 3) \\
&= \frac{1}{2} (1 - p_t)^2 - \frac{1}{2} F_{h_1+h_2}(t),
\end{aligned}$$

where

$$F_{h_1+h_2}(t) := \mathbf{P}(h_1 + h_2 < t \mid \deg_T(x) = 3) = \int_0^t \ell * \ell(y) dy.$$

The Laplace transform of p_t is known to be

$$\begin{aligned}
\mathcal{L}p(s) &= \frac{1}{\sqrt{(\lambda + s)^2 - \lambda^2}} + \frac{\lambda}{\sqrt{(\lambda + s)^2 - \lambda^2}(\lambda + s + \sqrt{(\lambda + s)^2 - \lambda^2})} \\
&= \frac{1}{s} - \frac{\lambda}{s(\lambda + s + \sqrt{(\lambda + s)^2 - \lambda^2})} = \frac{1}{s} - \frac{1}{s} \mathcal{L}\ell(s).
\end{aligned}$$

Thus, by (11),

$$(21) \quad \mathcal{L}p(s) = \frac{1}{2s} + \frac{1}{\lambda} \mathcal{L}\ell(s) - \frac{1}{2s} (\mathcal{L}\ell(s))^2.$$

Hence, the Laplace transform of $F_{h_1+h_2}(t)$ is

$$\begin{aligned}
\mathcal{L}F_{h_1+h_2}(s) &= \frac{1}{s} \int_0^\infty e^{-st} \ell * \ell(t) dt = \frac{1}{s} (\mathcal{L}\ell(s))^2 \\
&= \frac{1}{s} + \frac{2}{\lambda} \mathcal{L}\ell(s) - 2\mathcal{L}p(s).
\end{aligned}$$

Therefore,

$$F_{h_1+h_2}(t) = 1 + \frac{2}{\lambda} \ell(t) - 2p_t$$

and

$$\begin{aligned}
(22) \quad \mathbf{P}(\deg_T(x) = 3 \text{ and } h_1 \vee h_2 \leq t < h_1 + h_2) &= \frac{1}{2} (1 - p_t)^2 - \frac{1}{2} F_{h_1+h_2}(t) \\
&= \frac{p_t^2}{2} - \frac{1}{\lambda} \ell(t).
\end{aligned}$$

Case IV

$$\begin{aligned}
& \mathbf{P}(\deg_T(x) = 3 \text{ and } h_1 + h_2 \leq t < X + h_1 + h_2) \\
&= \frac{1}{2} \mathbf{P}(h_1 + h_2 \leq t < X + h_1 + h_2 \mid \deg_T(x) = 3) \\
&= \frac{1}{2} \int_0^t e^{-\lambda(t-y)} \ell * \ell(y) dy \\
(23) \quad &= \frac{1}{2\lambda} \phi_\lambda * \ell * \ell(t) = \frac{1}{\lambda} \ell(t) - \frac{1}{2\lambda} \phi_\lambda(t)
\end{aligned}$$

by (10).

Case V

$$(24) \quad \mathbf{P}(\deg_T(x) = 1 \text{ and } t < X) = \frac{1}{2} \mathbf{P}(t < X) = \frac{1}{2} e^{-\lambda t} = \frac{1}{2\lambda} \phi_\lambda(t).$$

Alternatively, the sum of the probabilities in cases IV and V can be computed as

$$\int_0^\infty e^{-\lambda y} \ell(t) dy = \frac{1}{\lambda} \ell(t),$$

which is consistent with (23) and (24).

Observe that the probabilities in (19), (20), (22), (23), and (24) add up to

$$p_t = \mathbf{P}(\mathcal{S}_t(\varphi, T) \neq \phi).$$

To prove part (ii), observe that the probabilities in (23) and (24) add up to $\frac{1}{\lambda} \ell(t)$, while the probabilities in (22), (23), and (24) add up to $\frac{p_t^2}{2}$. Thus the fraction of leaves with single sink is $\frac{1}{\lambda} \ell(t) / \frac{p_t^2}{2}$.

By construction, each single mass at a leaf has mass $2t$. For a double mass, (22) implies the following cumulative distribution function for

positive a and b satisfying $a \vee b \leq 2t < a + b$.

$$\begin{aligned}
& F(a, b) \\
&= \frac{\mathbf{P}(\deg_T(x) = 3, h_1 \leq a/2, h_2 \leq b/2, t < h_1 + h_2 \mid \mathcal{S}_t(\varphi, T) \neq \phi)}{p_t^2 - \frac{1}{\lambda}\ell(t)} \\
&= \frac{\int_0^{a/2} \mathbf{P}(t - y < h_2 \leq b/2 \mid \mathcal{S}_t(\varphi, T) \neq \phi \text{ and } \deg_T(x) = 3) \ell(y) dy}{p_t^2 - \frac{2}{\lambda}\ell(t)} \\
&= \frac{\int_0^{a/2} (p_{t-y} - p_{b/2}) \ell(y) dy}{p_t^2 - \frac{2}{\lambda}\ell(t)} \\
&= \frac{\int_0^{a/2} p_{t-y} \ell(y) dy - p_{b/2}(1 - p_{a/2})}{p_t^2 - \frac{2}{\lambda}\ell(t)}.
\end{aligned}$$

Differentiating, we obtain the statement of part (iii):

$$f(a, b) = \frac{\partial^2}{\partial a \partial b} F(a, b) = \frac{\frac{1}{4}\ell(a/2)\ell(b/2)}{p_t^2 - \frac{2}{\lambda}\ell(t)}.$$

For part (iv) observe that by (20),

$$\mathbf{P}(\deg_T(x) = 3 \text{ and } h_1 \wedge h_2 \leq t < h_1 \vee h_2 \mid \mathcal{S}_t(\varphi, T) \neq \phi) = 1 - p_t.$$

Thus each edge in $\mathcal{S}_t(\varphi, T)$ is partitioned into subintervals whose lengths are independent exponential random variables with parameter λ . The number of the subintervals is a geometric random variable with parameter p_t . At every point that separates a pair of adjacent subintervals there exists a mass, which can have either left or right orientation independently with probability $1/2$.

Finally, for $a \in (0, 2t)$, (20) implies

$$\begin{aligned}
& \frac{\mathbf{P}(\deg_T(x) = 3 \text{ and } h_1 \wedge h_2 \leq a/2 < t < h_1 \vee h_2 \mid \mathcal{S}_t(\varphi, T) \neq \phi)}{p_t(1 - p_t)} \\
&= \frac{\mathbf{P}(h_1 \leq a/2 < t < h_2 \mid \mathcal{S}_t(\varphi, T) \neq \phi \text{ and } \deg_T(x) = 3)}{p_t(1 - p_t)} \\
&= \frac{p_t(1 - p_{a/2})}{p_t(1 - p_t)} = \frac{1 - p_{a/2}}{1 - p_t}.
\end{aligned}$$

Next, we differentiate to obtain the p.d.f. for the mass of an interior sink, as in part (v),

$$\frac{d}{da} \frac{1 - p_{a/2}}{1 - p_t} = \frac{\ell(a/2)}{2(1 - p_t)}.$$

□

6. RANDOM SINK IN AN INFINITE EXPONENTIAL POTENTIAL

Here we focus on the dynamics of a random sink in the case of a negative exponential excursion potential. To avoid subtle conditioning related to a finite potential from $\widetilde{\mathcal{E}}^{\text{ex}}([a, b])$, we consider space $\widetilde{\mathcal{E}}^{\text{ex}}(\mathbb{R})$ of infinite potentials. Specifically, we consider here an infinite exponential potential $\Psi_0^{\text{exp}}(x)$, $x \in \mathbb{R}$, constructed as follows. Let x_i , $i \in \mathbb{Z}$ be the epochs of a Poisson point process on \mathbb{R} with rate $\lambda/2$, indexed so that x_0 is the epoch closest to the origin. The initial velocity $v(x, 0)$ is a piece-wise constant continuous function that alternates between values ± 1 within the intervals $(x_i - 1, x_i]$ and with $v(x_0, 0) = 1$. Accordingly, the initial potential $\Psi_0^{\text{exp}}(x)$ is a piece-wise linear continuous function with a local minimum at x_0 and alternating slopes ± 1 of independent exponential duration. The results in this section refer to the sink \mathcal{M}_0 with initial Lagrangian coordinate x_0 . We refer to \mathcal{M}_0 as a *random sink*, using translation invariance of Poisson point process.

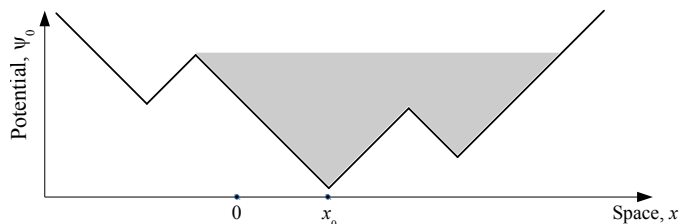


FIGURE 17. Random sink \mathcal{M}_0 . The particle \mathcal{M}_0 originates at point x_0 – the local minimum closest to the origin. Its dynamics during the time interval $[0, t]$ is completely specified by the finite negative excursion \mathcal{B}_0^t highlighted in the figure.

Observe that for any fixed $t > 0$, the dynamics of \mathcal{M}_0 is completely specified by a finite excursion within $\Psi_0^{\text{exp}}(x)$. For instance, one can consider the shortest negative excursion of $\Psi_0^{\text{exp}}(x)$ within interval \mathcal{B}_0^t such that $x_0 \in \mathcal{B}_0^t$, $|\mathcal{B}_0^t| > 2t$, and one end of \mathcal{B}_0^t is a local maximum of $\Psi_0^{\text{exp}}(x)$ (see Fig. 17). The respective Harris path is an exponential Galton-Watson tree $\text{GW}(\lambda)$. Lemma 5 implies that the dynamics of \mathcal{M}_0 consists of alternating intervals of mass accumulation (vertical

segments of $\mathcal{G}^{(x,\psi)}$) and motion (horizontal segments of $\mathcal{G}^{(x,\psi)}$), starting with a mass accumulation interval. Label the lengths v_i of the vertical segments and the lengths h_i of the horizontal segments in the order of appearance in the examined trajectory. Corollary 3 implies that v_i, h_i are independent; the lengths of v_i are independent identically distributed exponential random variables with parameter λ ; and the lengths of h_i equal the total lengths of independent Galton-Watson trees $\text{GW}(\lambda)$. This description, illustrated in Fig. 18, allows us to find the mass dynamics of a random sink.

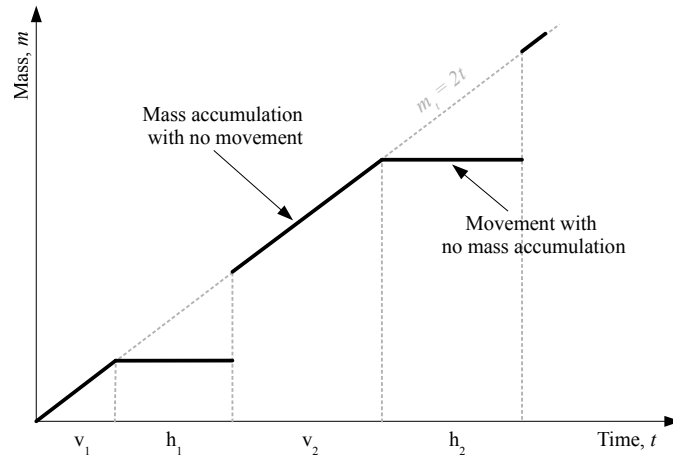


FIGURE 18. Dynamics of a random sink: an illustration. The trajectory of a sink is partitioned into alternating intervals of mass accumulation of duration v_i and intervals of movement with no mass accumulation of duration h_i . Each v_i is an exponential random variable with parameter λ . Each h_i is distributed as the total length of a critical Galton-Watson tree with exponential edge lengths with parameter λ .

Theorem 7 (Growth probability of a random sink). *The probability $\xi(t)$ that a random sink \mathcal{M}_0 is growing at a given instant $t > 0$ (that is, it is at rest and accumulates mass) is given by*

$$(25) \quad \xi(t) = e^{-\lambda t} I_0(\lambda t).$$

Proof. Let v_i , $i \geq 1$ be independent exponential random variables with parameter λ , and h_i , $i \geq 1$ be the total lengths of independent $\text{GW}(\lambda)$ trees. The sum $v_1 + \dots + v_k$ has the gamma density $\gamma_{\lambda,k}(x) = \frac{1}{(k-1)!} \lambda(\lambda x)^{k-1} e^{-x}$. The probability $\xi(t)$ that a random sink

is growing at a given instant $t > 0$ is

$$\begin{aligned}
\xi(t) &:= \mathbb{P}(\text{ a random sink is growing at instant } t) \\
&= \sum_{k=1}^{\infty} \mathbb{P} \left(\sum_{i=1}^{k-1} [v_i + h_i] < t < v_k + \sum_{i=1}^{k-1} [v_i + h_i] \right) \\
&= \sum_{k=1}^{\infty} \int_0^t \left(\int_{t-x}^{\infty} \lambda e^{-\lambda y} dy \right) \gamma_{k-1} * \ell_{k-1}(x) dx \\
(26) \quad &= \sum_{k=1}^{\infty} \int_0^t e^{-\lambda(t-x)} \gamma_{k-1} * \ell_{k-1}(x) dx = \frac{1}{\lambda} \sum_{k=1}^{\infty} \gamma_k * \ell_{k-1}(t),
\end{aligned}$$

where

$$\ell_k(x) = \underbrace{\ell * \dots * \ell}_{k \text{ times}}(x).$$

We calculate the Laplace transform $\mathcal{L}\xi(s)$ of the probability $\xi(t)$ in (26) as follows. We use the formula for the Laplace transform of $\ell(x)$ derived in (9) and (26) to obtain

$$\begin{aligned}
\mathcal{L}\xi(s) &= \frac{1}{\lambda} \sum_{k=1}^{\infty} \left(\frac{\lambda}{\lambda + s} \right)^k \left(\mathcal{L}\ell(s) \right)^{k-1} = \frac{1}{\lambda + s - \lambda \mathcal{L}\ell(s)} \\
(27) \quad &= \frac{1}{\lambda + s - \frac{\lambda^2}{\lambda + s + \sqrt{(\lambda + s)^2 - \lambda^2}}} = \frac{1}{\sqrt{(\lambda + s)^2 - \lambda^2}}.
\end{aligned}$$

Finally, we use formula 29.3.93 in [2] to invert the Laplace transform in (27), and obtain

$$\xi(t) = e^{-\lambda t} I_0(\lambda t).$$

□

Theorem 8 (Mass distribution of a random sink). *The mass of a random sink \mathcal{M}_0 at instant $t > 0$ has probability distribution*

$$\begin{aligned}
\mu_t(a) &= \mathbf{1}_{(0,2t)}(a) \cdot \frac{\lambda}{2} e^{-\lambda t} \left[I_0(\lambda(t - a/2)) + I_1(\lambda(t - a/2)) \right] \cdot I_0(\lambda a/2) \\
(28) \quad &+ e^{-\lambda t} I_0(\lambda t) \delta_{2t}(a),
\end{aligned}$$

where δ_{2t} denotes Dirac delta function (point mass) at $2t$.

Proof. Let m_t denote the mass of a random sink at a fixed instant $t > 0$. When the sink is not growing, its mass m_t is strictly smaller than $2t$.

Then for any positive $a < 2t$,

$$\begin{aligned} \mathbf{P}(m_t \leq a) &= \sum_{k=1}^{\infty} \mathbf{P} \left(-h_k + \sum_{i=1}^k [v_i + h_i] \leq \frac{a}{2} < t < \sum_{i=1}^k [v_i + h_i] \right) \\ &= \sum_{k=1}^{\infty} \int_0^{a/2} \left(\int_{t-x}^{\infty} \ell(y) dy \right) \gamma_k * \ell_{k-1}(x) dx, \end{aligned}$$

and the corresponding density will be

$$\begin{aligned} \frac{d}{da} \mathbf{P}(m_t \leq a) &= \frac{1}{2} \int_{t-a/2}^{\infty} \ell(y) dy \cdot \sum_{k=1}^{\infty} \gamma_k * \ell_{k-1}(a/2) \\ &= \frac{\lambda}{2} \int_{t-a/2}^{\infty} \ell(y) dy \cdot \xi(a/2) \\ &= \frac{\lambda}{2} e^{-\lambda(t-a/2)} \left[I_0(\lambda(t-a/2)) + I_1(\lambda(t-a/2)) \right] \cdot e^{-\lambda a/2} I_0(\lambda a/2) \\ &= \frac{\lambda}{2} e^{-\lambda t} \left[I_0(\lambda(t-a/2)) + I_1(\lambda(t-a/2)) \right] \cdot I_0(\lambda a/2) \end{aligned}$$

by (13) and (25). Thus, the distribution of the mass of a random sink at instant t is given by

$$\begin{aligned} \mu_t(a) &= \mathbf{1}_{(0,2t)}(a) \cdot \frac{d}{da} \mathbf{P}(m_t \leq a) + \xi(t) \delta_{2t}(a) \\ &= \mathbf{1}_{(0,2t)}(a) \cdot \frac{\lambda}{2} e^{-\lambda t} \left[I_0(\lambda(t-a/2)) + I_1(\lambda(t-a/2)) \right] \cdot I_0(\lambda a/2) \\ &\quad + e^{-\lambda t} I_0(\lambda t) \delta_{2t}(a), \end{aligned}$$

where δ_{2t} denotes Dirac delta function (point mass) at $2t$. \square

7. DISCUSSION

This paper introduces a generalized dynamical pruning of binary rooted trees (Section 2.2) that encompasses several pruning operations discussed in the probability literature, notably including the tree erasure from leaves at a constant rate of Example 1 [29, 15, 10] and Horton pruning of Example 2 [31, 9, 26]. Curiously, these two examples seem to be the only cases when the pruning satisfies the semigroup property (either in discrete or continuous time). The other natural pruning operations, like pruning by the total tree length (Example 3) or by the number of leaves (Example 4), do not have the semigroup property. The absence of semigroup property is related to the existence

of discontinuities of a respective pruning function $\varphi(T)$ along a tree $T \in \mathcal{L}_{\text{plane}}$. It would be interesting to find the necessary and sufficient conditions on $\varphi(T)$ for the existence or absence of the semigroup property.

Measures invariant with respect to the generalized pruning (Section 2.4, Definition 1) seem to be abundant on $\mathcal{L}_{\text{plane}}$. The critical binary Galton-Watson tree $\text{GW}(\lambda)$ with i.i.d. exponential edge lengths, a traditional subject of invariance studies, is shown here to be prune invariant under an arbitrary choice of the pruning function (Section 3.5, Theorem 2). The work [26] shows how to construct a variety of measures invariant with respect to the Horton pruning (for combinatorial trees); it is very likely that this approach can be modified to include edge lengths and used for generating measures invariant with respect to other versions of the generalized pruning. An interesting problem is finding measures invariant with respect to multiple versions of pruning. At the moment the only known solution is the exponential critical binary Galton-Watson tree $\text{GW}(\lambda)$, invariant with respect to all admissible prunings. It seems that a family of critical Tokunaga trees, which is shown in [26] to be invariant with respect to the Horton pruning, is a promising candidate to be invariant with respect to other prunings.

Pruning might play a role in the analysis of dynamical systems, including the problem of finding self-similar or time-invariant solutions. As a motivational example, we show here (Section 4) that the dynamics of a ballistic annihilation model $A + A \rightarrow \emptyset$, well known in the physics literature, is equivalent to the generalized dynamical pruning of a particular class of trees (Section 4.4, Theorem 5). This tree-based interpretation of the model dynamics opens a way for a complete probabilistic description of model solutions (Section 5, Theorem 6), and finding the time evolution of selected statistics (Section 6, Theorem 7). It seems promising to expand the proposed analysis to other initial potentials, as well as to other particle systems known to be critically dependent on the shock dynamics. We observe, for instance, that the dynamics of particles in the ballistic annihilation model, prior to particle collision, coincides with that in the famous 1-D inviscid Burgers equation

$$\partial_t v(x, t) + v \partial_x v(x, t) = 0, \quad x \in \mathbb{R}, t \in \mathbb{R}_+,$$

which also describes the evolution of a velocity field $v(x, t)$. The Burgers dynamics appears in a surprising variety of problems, ranging from cosmology to fluid dynamics and vehicle traffic models; see [4, 18, 19] for comprehensive review. The Burgers equation produces shock waves

that correspond to the appearance of massive particles and can be represented as trees (analogously to the shock waves of sinks considered in this work). It would be interesting to explore if there exists a manageable relation between the initial Burgers velocity field $v(x, 0)$ and the respective shock wave tree, at least for special initial velocity fields, and if such trees are prune invariant for a suitable pruning function $\varphi(T)$.

ACKNOWLEDGEMENTS

We are grateful to Ed Waymire for his continuing support and encouragement. This research is supported by the NSF awards DMS-1412557 (Y.K.) and EAR-1723033 (I.Z.).

REFERENCES

- [1] R. Abraham, J.-F. Delmas, H. He, *Pruning Galton-Watson trees and tree-valued Markov processes* Ann. Inst. H. Poincaré Probab. Statist., **48**(3) (2012) 688–705.
- [2] M. Abramowitz and I. A. Stegun, *Handbook of mathematical functions: with formulas, graphs, and mathematical tables* Courier Corporation, **55** (1964).
- [3] D.J. Aldous, J. Pitman, *Tree-valued Markov chains derived from Galton-Watson processes* Ann. Inst. H. Poincaré Probab. Statist., **34**(5) (1998) 637–686.
- [4] J. Bec and K. Khanin, *Burgers turbulence* Physics Reports, **447**(1) (2007) 1–66.
- [5] E. Ben-Naim, S. Redner, and F. Leyvraz, *Decay kinetics of ballistic annihilation* Physical Review Letters, **70**(12) (1993) 1890–1893.
- [6] E. Ben-Naim, S. Redner, and P. L. Krapivsky, *Two scales in asynchronous ballistic annihilation* J. Phys. A: Math. Gen., **29** L561 (1996).
- [7] V. Belitsky and P. A. Ferrari, *Ballistic annihilation and deterministic surface growth* Journal of Statistical Physics, **80**(3-4) (1995) 517–543.
- [8] R. A. Blythe, M. R. Evans, and Y. Kafri, *Stochastic ballistic annihilation and coalescence* Physical Review Letters, **85**(18) (2000) 3750–3753.
- [9] G. A. Burd, E. C. Waymire and R. D. Winn, *A self-similar invariance of critical binary Galton-Watson trees* Bernoulli, **6** (2000) 1–21.
- [10] T. Duquesne and M. Winkel, *Hereditary tree growth and Levy forests* arXiv:1211.2179 (2012) preprint.
- [11] P. S. Dodds, D. H. Rothman, *Unified view of scaling laws for river networks* Phys. Rev. E, **59**(5) (1999) 4865.
- [12] M. Droz, P.-A. Rey, L. Frachebourg, and J. Piasecki, *Ballistic-annihilation kinetics for a multivelocity one-dimensional ideal gas* Phys. Rev. E **51**(6) (1995) 5541–5548.
- [13] Y. Elskens and H. L. Frisch, *Annihilation kinetics in the one-dimensional ideal gas* Physical Review A, **31**(6) (1985) 3812–3816.
- [14] A. Ermakov, B. Toth, and W. Werner, *On some annihilating and coalescing systems* Journal of Statistical Physics, **91**(5-6) (1998) 845–870.

- [15] S. N. Evans, *Probability and real trees: Ecole d'été de probabilités de Saint-Flour Lectures on Probability Theory and Statistics*. Springer (2008).
- [16] S. N. Evans, J. Pitman, and A. Winter, *Rayleigh processes, real trees, and root growth with re-grafting* *Probability Theory and Related Fields* **134**(1) (2006) 81–126.
- [17] P. Flajolet, J.-C. Raoult, J. Vuillemin, *The number of registers required for evaluating arithmetic expressions* *Theoretical Computer Science* **9**(1) (1979) 99–125.
- [18] U. Frisch, J. Bec, and B. Villone, *Singularities and the distribution of density in the Burgers/adhesion model* *Physica D*, **152/153** (2001) 620–635.
- [19] S. Gurbatov, A. Malakhov, and A. Saichev, *Nonlinear random waves and turbulence in nondispersive media: waves, rays, particles* Manchester University Press, Manchester, (1991)
- [20] T. E. Harris, *First passage and recurrence distribution* *Trans. Amer. Math. Soc.*, **73** (1952) 471–486.
- [21] A. Katok and B. Hasselblatt, *Introduction to the modern theory of dynamical systems* Vol. 54. Cambridge university press (1997).
- [22] J. W. Kirchner, *Statistical inevitability of Horton's laws and the apparent randomness of stream channel networks* *Geology*, **21**(7) (1993) 591–594.
- [23] Y. Kovchegov and I. Zaliapin, *Horton Law in Self-Similar Trees* *Fractals*, Vol. 24, No. 2 (2016) 1650017.
- [24] Y. Kovchegov and I. Zaliapin, *Horton self-similarity of Kingman's coalescent tree* *Ann. Inst. H. Poincaré Probab. Statist.*, **53**(3) (2017) 1069–1107.
- [25] Y. Kovchegov and I. Zaliapin, *Tokunaga self-similarity arises naturally from time invariance* *Chaos: An Interdisciplinary Journal of Nonlinear Science*, **28**(4) (2018) 041102.
- [26] Y. Kovchegov and I. Zaliapin, *Random self-similar trees and a hierarchical branching process* *Stochastic Processes and Their Applications*, to appear (2018) arXiv:1608.05032.
- [27] P. L. Krapivsky, S. Redner, and E. Ben-Naim, *A kinetic view of statistical physics* Cambridge University Press (2010).
- [28] J. F. Le Gall, *The uniform random tree in a Brownian excursion* *Probab. Theory Relat. Fields*, **96** (1993) 369–383.
- [29] J. Neveu, *Erasing a branching tree* *Advances in applied probability*, **1** (1986) 101–108.
- [30] J. Neveu and J. Pitman, *Renewal property of the extrema and tree property of the excursion of a one-dimensional Brownian motion* *Séminaire de Probabilités XXIII*, **1372** of the series *Lecture Notes in Mathematics*, (1989) 239–247.
- [31] S. D. Peckham, *New results for self-similar trees with applications to river networks* *Water Resources Res.* **31** (1995) 1023–1029.
- [32] J. Piasecki, *Ballistic annihilation in a one-dimensional fluid* *Phys.Rev. E* **51**(6) (1995) 5535–5540.
- [33] J. Pitman, *Combinatorial Stochastic Processes: Ecole d'été de probabilités de Saint-Flour XXXII-2002 Lectures on Probability Theory and Statistics*. Springer. Available at <http://stat.berkeley.edu/users/pitman/621.pdf>, (2006).
- [34] V. Sidoravicius and L. Tournier, *Note on a one-dimensional system of annihilating particles* *Electron. Commun. Probab.*, **22**(59) (2017) 1–9.

- [35] D. G. Tarboton, *Fractal river networks, Horton's laws and Tokunaga cyclicity* Journal of hydrology, **187**(1) (1996) 105–117.
- [36] I. Zaliapin and Y. Kovchegov, *Tokunaga and Horton self-similarity for level set trees of Markov chains* Chaos, Solitons & Fractals, **45**(3) (2012) 358–372.
- [37] S. Zanardo, I. Zaliapin, and E. Foufoula-Georgiou, *Are American rivers Tokunaga self-similar? New results on fluvial network topology and its climatic dependence* J. Geophys. Res., **118** (2013) 166–183.

DEPARTMENT OF MATHEMATICS, UNIVERSITY OF TEXAS AT DALLAS, RICHARDSON, TX, USA

E-mail address: maxim.arnold@utdallas.edu

DEPARTMENT OF MATHEMATICS, OREGON STATE UNIVERSITY, CORVALLIS, OR, USA

E-mail address: kovchegy@math.oregonstate.edu

DEPARTMENT OF MATHEMATICS AND STATISTICS, UNIVERSITY OF NEVADA, RENO, NV, USA

E-mail address: zal@unr.edu